Contemporary Mathematics
https://ojs.wiserpub.com/index.php/CM/

Research Article

Emergence of Complex Wave Structures and Stability Analysis for (3 + 1)-Dimensional Generalized *B*-Type Kadomtsev-Petviashvili Equation with *M*-Fractional Derivative Using Advanced Technique

M. Elsaid Ramadan[1], Mohammed S. Ghayad[2*], Hamdy M. Ahmed[3], Niveen M. Badra[2], Wafaa B. Rabie[4]

[1] Department of Mathematics, Faculty of Science, Islamic University of Madinah, Medina, Saudi Arabia
[2] Department of Physics and Engineering Mathematics, Faculty of Engineering, Ain Shams University, Abbassia, Cairo, Egypt
[3] Department of Physics and Engineering Mathematics, Higher Institute of Engineering, El Shorouk Academy, Cairo, Egypt
[4] Department of Mathematics, Faculty of Science, Luxor University, Taiba, Luxor, Egypt
E-mail: m.elsayed@eng.asu.edu.eg

Received: 4 July 2025; **Revised:** 16 August 2025; **Accepted:** 25 August 2025

Abstract: This study investigates the fractional $(3+1)$-dimensional Generalized *B*-type Kadomtsev-Petviashvili Equation (GBKPE) using the Modified Extended Mapping Method (MEMM). The model plays a fundamental role in describing nonlinear wave propagation in fluid dynamics and other complex media, particularly the evolution of three-dimensional surfaces, shallow water waves, and diverse physical phenomena. By incorporating the local *M*-fractional derivative, the equation captures non-local interactions and memory effects—features inaccessible to classical derivatives—making it ideal for modeling long-range disturbances and hereditary properties. The primary objective is to derive novel exact solutions exhibiting complex dynamics in higher dimensions. Through MEMM, we obtain a wide range of solutions, including dark and singular solitons, Jacobi elliptic functions, hyperbolic, exponential, and singular periodic waves. Notably, some solutions exhibit previously unreported characteristics, underscoring the method's innovation. We analyze the impact of fractional parameters on wave profiles, supported by 2D, 3D, and contour plots to visualize their dynamic behavior. A linear stability analysis further confirms the robustness of key solutions under small perturbations, ensuring their physical relevance. The results demonstrate the efficacy of MEMM in solving fractional GBKPE, significantly expanding the known analytical solutions. This work not only advances the understanding of multidimensional nonlinear equations but also provides a foundation for future studies in wave dynamics, stability, and applications to real-world systems like plasma physics and nonlinear optics.

***Keywords*:** generalized Kadomtsev-Petviashvili equation, fractional calculus, modified extended mapping method, nonlinear wave solutions, soliton stability, *M*-fractional derivative, wave propagation dynamics

MSC: 35C07, 35C08, 35C09

DOI: https://doi.org/10.37256/cm.6520257717

1. Introduction

The Nonlinear Evolution Equations (NLEEs) provide accurate descriptions and simulations for nonlinear processes that appear in domains including engineering, physics, computational mathematics, chemistry, and biological science. Exploring traveling wave solutions offers important insights into the behavior of different physical systems. Utilizing either analytical or numerical methods, these solutions enhance our understanding of wave dynamics across various contexts, establishing them as a crucial focus in applied mathematics and physics [1–16]. Through the application of diverse mathematical techniques to identify and examine these solutions, researchers can reveal the fundamental mechanisms influencing complex systems [17–25].

In recent years, fractional calculus has become increasingly interesting to researchers because of its broad applicability across various fields. Unlike traditional derivatives, fractional derivatives are characterized by their non-local properties and ability to retain historical information [26, 27]. It is worth noting that different definitions of fractional derivatives, such as Caputo, Riemann, Liouville and Hadamard forms, could also be employed to model memory effects in nonlinear optical systems [28–30]. However, these types often involve nonlocal integral kernels, which increase computational complexity and storage requirements in both analytical and numerical treatments. Also, these types use an integral form for the fractional derivative and do not satisfy the main properties of ordinary integer derivatives, such as the chain rule, product rule, and quotient rule. On the other hand, there are new kinds of fractional derivative which were presented by some authors, such as conformable fractional derivatives [31], beta-fractional derivative [32], and M-fractional derivative [33]. These novel operators have attracted considerable attention because they overcome some of the limitations of the classical definitions of fractional derivatives. In particular, they provide more flexibility in modeling complex phenomena, preserve certain desirable properties of the standard derivative, and can be effectively applied to various classes of nonlinear partial differential equations. Consequently, these derivatives have become an active area of research, with applications ranging from mathematical physics and and applied sciences (see [34–36]). Several analytical and numerical approaches have been used to obtain solutions for fractional differential equations, such as the homotopy analysis method [37], the Lagrange characteristic method [38], modified simple equation method [39], and the differential transformation method [40]. Talra et al. used the Jacobi elliptic function technique to investigate solitary wave solutions associated with the perturbed Chen-Lee-Liu equation [41].

A (3 + 1)-dimensional Generalized B-type Kadomtsev-Petviashvili Equation (GBKPE) was recently introduced to describe the propagation of shallow water waves in water canals [33]. This generalized form enhances the GBKPE equation's ability to capture various wave phenomena and interactions, including anisotropy effects and higher-order nonlinearities. The GBKPE has been studied through a considerable amount of research work. Ma et al. [42] extracted a breather-travelling-wave solution, a kink soliton for GBKPE. Jian et al. [43] developed one- and two-periodic solutions by utilizing the Riemann theta function for GBKPE. Ghayad et al. [44] solved the GBKPE using the improved modified extended tanh function method to extract its exact solutions. While Yan et al. [45] obtained the GBKPE's one- and two-soliton solutions by using Hirota's bilinear approach.

In the present study, we consider the fractional (3 + 1)-dimensional GBKPE:

$$D_{M,t}^{\sigma,\omega}(\psi_x+\psi_y+\psi_z)+\zeta\psi_{xxxy}+\beta\left(\psi_x\psi_y\right)_x+\gamma\psi_{xx}+\delta\psi_{zz}=0, \tag{1}$$

where $\psi(x, y, z, t)$ is a real differentiable function of the spatial coordinates x, y, z and temporal coordinate t, ζ denotes dispersion coefficient, β represents the nonlinearity coefficient, γ represents the second-order x-direction diffusion coefficient, δ represents the second-order z-direction diffusion coefficient, the subscripts denote the partial derivatives, and $D_{M,t}^{\sigma,\omega}$ denotes the M-fractional derivative of order σ with the following definition [33].

$$D_{M}^{\sigma,\omega}\psi(t)=\lim_{\varepsilon\to 0}\frac{\psi(tE_{\omega}(\varepsilon t^{-\sigma}))-\psi(t)}{\varepsilon},\quad t>0, \tag{2}$$

where $0 < \sigma \leq 1$, M shows the derived function includes a function called Mittag Leffler $E_{\omega}(.)$ with one parameter $\omega > 0$:

$$E_{\omega}(Z) = \sum_{k=0}^{\infty} \frac{Z^k}{\Gamma(\omega k + 1)}. \tag{3}$$

When $\sigma = \omega = 1$, the original form of the (3 + 1)-dimensional (GBKP) equation is obtained [42].

In this study, the Modified Extended Mapping Method (MEMM) is employed for the first time to analyze the proposed model incorporating a local M-fractional derivative. The (3 + 1)-dimensional GBKPE is a generalized nonlinear wave equation that goes beyond classical integrable models in order to capture intricate multidimensional interactions, including those appearing in fluid dynamics, nonlinear optics, and plasma physics. Its multidimensionality makes it especially well-adapted to model wave propagation phenomena in which the interactions take place in more than one spatial direction, and in which time-dependent dispersion and nonlinearity play a crucial role. The implementation of fractional derivatives, especially the local M-derivative, is motivated by the need to describe memory effects and hereditary characteristics of physical systems that are not accounted for by traditional integer-order derivatives. Fractional operators, in contrast to classical derivatives, enable the more flexible and realistic modeling of nonlocal interactions, anomalous diffusion, and wave attenuation. The local M-derivative, specifically, provides a computationally physically appealing framework, maintaining locality while retaining the spirit of fractional-order dynamics. By using the fractional local M-derivative in the GBKPE model, we obtain a more realistic and useful mathematical model for simulating real-world phenomena in which long-range dependence and memory are essential features. It also makes the model more flexible for practical use in nonlinear acoustic waves, geophysical fluid dynamics, and signal transmission in complicated media. The primary novelty of this research is to discover new, distinct solutions for the proposed model that have not been reported in previous studies. The suggested method was chosen over others due to its ability to generate a wider variety of complex solutions, making it particularly effective for addressing various types of Nonlinear Partial Differential Equations (NLPDEs). Consequently, new solutions, including Jacobi elliptic functions, dark and singular soliton wave solutions, as well as hyperbolic, exponential, and singular periodic solutions, were successfully derived. These findings demonstrate the efficiency and robustness of the mentioned approach. To demonstrate the true physical behavior of the model, contour, 2D, and 3D charts are also displayed.

The manuscript is organized as follows: A synopsis of the recommended approach is provided in Section 2. The application of the recommended approach to the suggested model and the extraction of its solution are covered in Section 3. While Section 4 presents results and a Discussion of some obtained solutions. Stability analysis of the fractional PDE in Section 5. A number of solutions are presented using graphical representations in Section 6. The work's conclusion is provided in Section 7. Lastly, a future recommendation is introduced in Section 8.

2. Overview of the methodology

This part presents a comprehensive outline of the MEMM (see [46, 47]). The general form of NLPDE is:

$$G\left(\psi, D_{M,t}^{\sigma,\omega}\psi, \psi_x, \psi_y, \psi_z, \psi_{xx}, \psi_{yy}, \psi_{zz}, \psi_{xt}, ...\right) = 0. \tag{4}$$

Algorithm 1 Assuming the solution of the previous equation is given as follows:

$$\psi(x, y, z, t) = \mathscr{W}(\xi), \qquad \xi = \lambda_1 x + \lambda_2 y + \lambda_3 z + \lambda_4 \frac{\Gamma(\omega + 1)t^{\sigma}}{\sigma}, \tag{5}$$

where λ_1, λ_2 and λ_3 are the wave number, while λ_4 is the soliton frequency, and $0 < \sigma \leq 1$.

So, Eq. (4) can be rewritten as:

$$R(\mathscr{W}, \mathscr{W}', \mathscr{W}'', \ldots) = 0. \tag{6}$$

Algorithm 2 The following expression is regarded as the cornerstone of the solution to the Eq. (6):

$$\mathscr{W}(\xi) = \sum_{i=0}^{N} f_i \Theta^i(\xi) + \sum_{i=-1}^{-N} g_{-i} \Theta^i(\xi) + \sum_{i=2}^{N} h_i \Theta^{i-2}(\xi)\Theta'(\xi) + \sum_{i=-1}^{-N} r_{-i} \Theta^i(\xi)\Theta'(\xi), \tag{7}$$

where Θ fulfills the subsequent auxiliary equation:

$$\Theta'(\xi) = \sqrt{\mathfrak{s}_0 + \mathfrak{s}_1\Theta(\xi) + \mathfrak{s}_2\Theta^2(\xi) + \mathfrak{s}_3\Theta^3(\xi) + \mathfrak{s}_4\Theta^4(\xi) + \mathfrak{s}_6\Theta^6(\xi)}. \tag{8}$$

Eq. (8) exhibits the following cases for its solution:

Case 1 When $\mathfrak{s}_0 = \mathfrak{s}_1 = \mathfrak{s}_3 = \mathfrak{s}_6 = 0$, the next solutions are introduced:

$$\Theta(\xi) = \sqrt{-\frac{\mathfrak{s}_2}{\mathfrak{s}_4}} \sec\left[\xi\sqrt{-\mathfrak{s}_2}\right], \quad \mathfrak{s}_2 < 0,\ \mathfrak{s}_4 > 0,$$

$$\Theta(\xi) = \sqrt{-\frac{\mathfrak{s}_2}{\mathfrak{s}_4}} \csc\left[\xi\sqrt{-\mathfrak{s}_2}\right], \quad \mathfrak{s}_2 < 0,\ \mathfrak{s}_4 > 0,$$

$$\Theta(\xi) = \sqrt{-\frac{\mathfrak{s}_2}{\mathfrak{s}_4}} \operatorname{sech}\left[\xi\sqrt{\mathfrak{s}_2}\right], \quad \mathfrak{s}_2 > 0,\ \mathfrak{s}_4 < 0.$$

Case 2 When $\mathfrak{s}_1 = \mathfrak{s}_3 = \mathfrak{s}_6 = 0$, $\mathfrak{s}_0 = \dfrac{\mathfrak{s}_2^2}{4\mathfrak{s}_4}$, the following solutions are brought up:

$$\Theta(\xi) = \sqrt{\frac{-\mathfrak{s}_2}{2\mathfrak{s}_4}} \tanh\left[\xi\sqrt{\frac{-\mathfrak{s}_2}{2}}\right], \quad \mathfrak{s}_2 < 0,\ \mathfrak{s}_4 > 0,$$

$$\Theta(\xi) = \sqrt{\frac{\mathfrak{s}_2}{2\mathfrak{s}_4}} \tan\left[\xi\sqrt{\frac{\mathfrak{s}_2}{2}}\right], \quad \mathfrak{s}_2 > 0,\ \mathfrak{s}_4 > 0.$$

Case 3 When $\mathfrak{s}_3 = \mathfrak{s}_4 = \mathfrak{s}_6 = 0$, the following solutions are brought up:

$$\Theta(\xi)=\sqrt{\frac{\mathfrak{s}_0}{\mathfrak{s}_2}}\sinh\left[\xi\sqrt{\mathfrak{s}_2}\right],\quad \mathfrak{s}_0>0,\ \mathfrak{s}_2>0,\ \mathfrak{s}_1=0,$$

$$\Theta(\xi)=\sqrt{-\frac{\mathfrak{s}_0}{\mathfrak{s}_2}}\sin\left[\xi\sqrt{-\mathfrak{s}_2}\right],\quad \mathfrak{s}_0>0,\ \mathfrak{s}_2<0,\ \mathfrak{s}_1=0,$$

$$\Theta(\xi)=-\frac{\mathfrak{s}_1}{2\mathfrak{s}_2}+e^{\xi\sqrt{\mathfrak{s}_2}},\quad \mathfrak{s}_2>0,\ \mathfrak{s}_0=\frac{\mathfrak{s}_1^2}{4\mathfrak{s}_2}.$$

Case 4 When $\mathfrak{s}_0=\mathfrak{s}_1=\mathfrak{s}_6=0$, the following solutions are brought up:

$$\Theta(\xi)=-\frac{\mathfrak{s}_2}{\mathfrak{s}_3}\left(\tanh\left[\frac{1}{2}\xi\sqrt{\mathfrak{s}_2}\right]+1\right),\quad \mathfrak{s}_2>0,\ \mathfrak{s}_3=\pm2\sqrt{\mathfrak{s}_2\mathfrak{s}_4},$$

$$\Theta(\xi)=-\frac{\mathfrak{s}_2}{\mathfrak{s}_3}\left(\coth\left[\frac{1}{2}\xi\sqrt{\mathfrak{s}_2}\right]+1\right),\quad \mathfrak{s}_2>0,\ \mathfrak{s}_3=\pm2\sqrt{\mathfrak{s}_2\mathfrak{s}_4}.$$

Case 5 When $\mathfrak{s}_1=\mathfrak{s}_3=0$, the following solutions are brought up:

$$\Theta(\xi)=\sqrt{\frac{2s_2\mathrm{sech}^2\left(\xi\sqrt{\mathfrak{s}_2}\right)}{2\sqrt{\mathfrak{s}_4^2-4\mathfrak{s}_2\mathfrak{s}_6}-\left(\sqrt{\mathfrak{s}_4^2-4\mathfrak{s}_2\mathfrak{s}_6}+\mathfrak{s}_4\right)\mathrm{sech}^2\left(\xi\sqrt{\mathfrak{s}_2}\right)}},\quad \mathfrak{s}_2>0,$$

$$\Theta(\xi)=\sqrt{\frac{2\mathfrak{s}_2\sec^2\left(\xi\sqrt{-\mathfrak{s}_2}\right)}{2\sqrt{\mathfrak{s}_4^2-4\mathfrak{s}_2\mathfrak{s}_6}-\left(\sqrt{\mathfrak{s}_4^2-4\mathfrak{s}_2\mathfrak{s}_6}-\mathfrak{s}_4\right)\sec^2\left(\xi\sqrt{-\mathfrak{s}_2}\right)}},\quad \mathfrak{s}_2<0.$$

Case 6 When $\mathfrak{s}_1=\mathfrak{s}_3=0$, the following solutions are brought up (Table 1):

Table 1. Jacobi elliptic function solutions

No.	$\mathfrak{s}_0$	$\mathfrak{s}_2$	$\mathfrak{s}_4$	$\Theta(\xi)$
1	1	$-1-\mathrm{m}^2$	m^2	$\mathrm{sn}(\omega,\mathrm{m})$ or $\mathrm{cd}(\omega,\mathrm{m})$
2	m^2-1	$2-\mathrm{m}^2$	-1	$\mathrm{dn}(\omega,\mathrm{m})$
3	$-\mathrm{m}^2$	$2\mathrm{m}^2-1$	$1-\mathrm{m}^2$	$\mathrm{nc}(\omega,\mathrm{m})$
4	-1	$2-\mathrm{m}^2$	m^2-1	$\mathrm{nd}(\omega,\mathrm{m})$
5	$\mathrm{m}^4-2\mathrm{m}^3+\mathrm{m}^2$	$-\frac{4}{\mathrm{m}}$	$-\mathrm{m}^2+6\mathrm{m}-1$	$\frac{\mathrm{mcn}(\omega\|\mathrm{m})\mathrm{dn}(\omega\|\mathrm{m})}{c\mathrm{sn}(\omega\|\mathrm{m})^2+1}$

Algorithm 3 By using Eq. (6) and the homogeneous balancing principle, the integer $\mathbb{N}$ will be determined.

Algorithm 4 Substituting Eq. (7) through Eq. (8) into Eq. (6) produces a polynomial in $\Theta(\xi)$. Subsequently, the sum of terms with equivalent power will be set to zero to form a system of nonlinear equations.

Algorithm 5 This system will be solved using Mathematica software.

3. Derivation of solutions

Initially, we will substitute by Eq. (3) into Eq. (1), hence Eq. (1) can be reformulated as follows:

$$\zeta\lambda_1^3\lambda_2\mathscr{W}^{(4)}+\left(\gamma\lambda_1^2+\delta\lambda_3^2+\lambda_1\lambda_4+\lambda_2\lambda_4+\lambda_3\lambda_4\right)\mathscr{W}''+2\beta\lambda_1^2\lambda_2\mathscr{W}'\mathscr{W}''=0. \tag{9}$$

Setting the integral constant to zero after integrating Eq. (7) once with respect to ξ will yield:

$$\zeta\lambda_1^3\lambda_2\mathscr{W}^{(3)}+\left(\gamma\lambda_1^2+\delta\lambda_3^2+\lambda_1\lambda_4+\lambda_2\lambda_4+\lambda_3\lambda_4\right)\mathscr{W}'+\beta\lambda_1^2\lambda_2\mathscr{W}'^2=0. \tag{10}$$

For simplicity, we assume that:

$$\mathscr{W}'(\xi)=H(\xi). \tag{11}$$

Therefore, Eq. (8) can be represented as follows:

$$\zeta\lambda_1^3\lambda_2H''+\left(\gamma\lambda_1^2+\delta\lambda_3^2+\lambda_1\lambda_4+\lambda_2\lambda_4+\lambda_3\lambda_4\right)H+\beta\lambda_1^2\lambda_2H^2=0. \tag{12}$$

Subsequently, the principle of balance is applied to Eq. (12) between H^2 and H'', which leads to the determination of $N=2$. As a result, the solution to Eq. (12) can be expressed as follows:

$$H(\xi)=f_0+f_1\Theta(\xi)+f_2\Theta(\xi)^2+\frac{g_1}{\Theta(\xi)}+\frac{g_2}{\Theta(\xi)^2}+h_2\Theta'(\xi)+r_1\frac{\Theta'(\xi)}{\Theta(\xi)}+r_2\frac{\Theta'(\xi)}{\Theta(\xi)^2}, \tag{13}$$

where f_0, f_1, f_2, g_1, g_2, h_2, r_1 and r_2 are constants that will be calculated, which f_2, g_2, h_2 and $r_2\neq0$ together.

Substituting Eq. (13) and Eq. (8) into Eq. (12), and subsequently equating the coefficients of terms with identical powers to zero, yields a system that will be solved using Mathematica software. This procedure allows us to determine the solutions of Eq. (1) with the constrain $\beta\neq0$ as shown below:

Case 1 $\mathfrak{s}_0=\mathfrak{s}_1=\mathfrak{s}_3=\mathfrak{s}_6=0$, we get $r_1=r_2=0$ and

(1.1) $f_0=f_1=0$, $f_2=-\dfrac{6\zeta\lambda_1\mathfrak{s}_4}{\beta}$, $g_1=g_2=h_2=0$, $\lambda_4=-\dfrac{\gamma\lambda_1^2+\delta\lambda_3^2+4\zeta\mathfrak{s}_2\lambda_2\lambda_1^3}{\lambda_1+\lambda_2+\lambda_3}$.

(1.2) $f_0=-\dfrac{4\zeta\lambda_1\mathfrak{s}_2}{\beta}$, $f_1=0$, $f_2=-\dfrac{6\zeta\lambda_1\mathfrak{s}_4}{\beta}$, $g_1=g_2=h_2=0$, $\lambda_4=-\dfrac{\gamma\lambda_1^2+\delta\lambda_3^2-4\mathfrak{s}_2\zeta\lambda_2\lambda_1^3}{\lambda_1+\lambda_2+\lambda_3}$.

In light of result (1.1), Eq. (1) will have the following solutions:

(1.1.1) If $\mathfrak{s}_2<0$ and $\mathfrak{s}_4>0$, singular periodic form solutions are presented as demonstrated:

$$\psi_{1.1.1}(x,y,z,t)=\frac{6\zeta\lambda_1\sqrt{-\mathfrak{s}_2}}{\beta}\tan\left[\left(\lambda_1x+\lambda_2y+\lambda_3z+\lambda_4\frac{\Gamma(\omega+1)t^\sigma}{\sigma}\right)\sqrt{-\mathfrak{s}_2}\right], \tag{14}$$

or

$$\psi_{1.1.1}(x,y,z,t) = -\frac{6\zeta\lambda_1\sqrt{-\mathfrak{s}_2}}{\beta}\cot\left[\left(\lambda_1 x+\lambda_2 y+\lambda_3 z+\lambda_4\frac{\Gamma(\omega+1)t^\sigma}{\sigma}\right)\sqrt{-\mathfrak{s}_2}\right]. \tag{15}$$

(1.1.2) If $\mathfrak{s}_2 > 0$ and $\mathfrak{s}_4 > 0$, dark soliton form solution is presented as demonstrated:

$$\psi_{1.1.2}(x,y,z,t) = \frac{6\zeta\lambda_1\sqrt{\mathfrak{s}_2}}{\beta}\tanh\left[\left(\lambda_1 x+\lambda_2 y+\lambda_3 z+\lambda_4\frac{\Gamma(\omega+1)t^\sigma}{\sigma}\right)\sqrt{\mathfrak{s}_2}\right]. \tag{16}$$

In light of result (1.2), Eq. (1) will have the following solutions:

(1.2.1) If $\mathfrak{s}_2 < 0$ and $\mathfrak{s}_4 > 0$, singular periodic kind are presented as demonstrated:

$$\psi_{1.2.1}(x,y,z,t) = -\frac{4\zeta\lambda_1\mathfrak{s}_2}{\beta}\left(\xi-\frac{3}{2\sqrt{-\mathfrak{s}_2}}\tan\left[\,\xi\sqrt{-\mathfrak{s}_2}\,\right]\right), \tag{17}$$

or

$$\psi_{1.2.1}(x,y,z,t) = -\frac{4\zeta\lambda_1\mathfrak{s}_2}{\beta}\left(\xi-\frac{3}{2\sqrt{-\mathfrak{s}_2}}\cot\left[\xi\sqrt{-\mathfrak{s}_2}\,\right]\right), \tag{18}$$

where $\xi = \lambda_1 x+\lambda_2 y+\lambda_3 z+\lambda_4\dfrac{\Gamma(\omega+1)t^\sigma}{\sigma}$.

(1.2.2) If $\mathfrak{s}_2 > 0$ and $\mathfrak{s}_4 > 0$, dark soliton form solution is presented as demonstrated:

$$\psi_{1.2.2}(x,y,z,t) = -\frac{4\zeta\lambda_1\mathfrak{s}_2}{\beta}\left(\xi-\frac{3}{2\sqrt{\mathfrak{s}_2}}\tanh\left[\xi\sqrt{\mathfrak{s}_2}\,\right]\right), \tag{19}$$

where $\xi = \lambda_1 x+\lambda_2 y+\lambda_3 z+\lambda_4\dfrac{\Gamma(\omega+1)t^\sigma}{\sigma}$.

Case 2 $\mathfrak{s}_1 = \mathfrak{s}_3 = \mathfrak{s}_6 = 0$, we get $f_1 = r_1 = h_2 = 0$ and

(2.1) $f_0 = -\dfrac{\zeta\lambda_1\mathfrak{s}_2}{\beta}$, $f_2 = -\dfrac{6\zeta\lambda_1\mathfrak{s}_4}{\beta}$, $g_1 = g_2 = r_2 = 0$, $\lambda_4 = -\dfrac{\gamma\lambda_1^2+\delta\lambda_3^2+2\zeta\mathfrak{s}_2\lambda_2\lambda_1^3}{\lambda_1+\lambda_2+\lambda_3}$.

(2.2) $f_0 = -\dfrac{\zeta\lambda_1\mathfrak{s}_2}{\beta}$, $f_2 = 0$, $g_1 = 0$, $g_2 = -\dfrac{3\zeta\lambda_1\mathfrak{s}_2^2}{2\beta\mathfrak{s}_4}$, $r_2 = 0$, $\lambda_4 = -\dfrac{\gamma\lambda_1^2+\delta\lambda_3^2+2\zeta\mathfrak{s}_2\lambda_2\lambda_1^3}{\lambda_1+\lambda_2+\lambda_3}$.

(2.3) $f_0 = \dfrac{2\zeta\lambda_1\mathfrak{s}_2}{\beta}$, $f_2 = -\dfrac{6\zeta\lambda_1\mathfrak{s}_4}{\beta}$, $g_1 = 0$, $g_2 = -\dfrac{3\zeta\lambda_1\mathfrak{s}_2^2}{2\beta\mathfrak{s}_4}$, $r_2 = 0$, $\lambda_4 = -\dfrac{\gamma\lambda_1^2+\delta\lambda_3^2+8\zeta\mathfrak{s}_2\lambda_2\lambda_1^3}{\lambda_1+\lambda_2+\lambda_3}$.

In light of result (2.1), Eq. (1) will have the following solutions:

(2.1.1) If $\mathfrak{s}_2 < 0$ and $\mathfrak{s}_4 > 0$, dark soliton form solution is presented as demonstrated:

$$\psi_{2.1.1}(x,y,z,t) = \frac{2\zeta\lambda_1\mathfrak{s}_2}{\beta}\left(\xi+\frac{3}{\sqrt{-2\mathfrak{s}_2}}\tanh\left[\xi\sqrt{-\frac{\mathfrak{s}_2}{2}}\right]\right), \tag{20}$$

where $\xi = \lambda_1 x+\lambda_2 y+\lambda_3 z+\lambda_4\dfrac{\Gamma(\omega+1)t^\sigma}{\sigma}$.

(2.1.2) If $\mathfrak{s}_2 > 0$ and $\mathfrak{s}_4 > 0$, singular periodic form solution is presented as demonstrated:

$$\psi_{2.1.2}(x, y, z, t) = \frac{2\zeta\lambda_1\mathfrak{s}_2}{\beta}\left(\xi - \frac{3}{\sqrt{2\mathfrak{s}_2}}\tan\left[\xi\sqrt{\frac{\mathfrak{s}_2}{2}}\right]\right), \tag{21}$$

where $\xi = \lambda_1 x + \lambda_2 y + \lambda_3 z + \lambda_4 \dfrac{\Gamma(\omega+1)t^\sigma}{\sigma}$.

In light of result (2.2), Eq. (1) will have the following solutions:

(2.2.1) If $\mathfrak{s}_2 < 0$ and $\mathfrak{s}_4 > 0$, singular soliton form solution is presented as demonstrated:

$$\psi_{2.2.1}(x, y, z, t) = \frac{2\zeta\lambda_1\mathfrak{s}_2}{\beta}\left(\xi + \frac{3}{\sqrt{-2\mathfrak{s}_2}}\coth\left[\xi\sqrt{-\frac{\mathfrak{s}_2}{2}}\right]\right), \tag{22}$$

where $\xi = \lambda_1 x + \lambda_2 y + \lambda_3 z + \lambda_4 \dfrac{\Gamma(\omega+1)t^\sigma}{\sigma}$.

(2.2.2) If $\mathfrak{s}_2 > 0$ and $\mathfrak{s}_4 > 0$, singular periodic form solution is presented as demonstrated:

$$\psi_{2.2.2}(x, y, z, t) = \frac{2\zeta\lambda_1\mathfrak{s}_2}{\beta}\left(\xi + \frac{3}{\sqrt{2\mathfrak{s}_2}}\cot\left[\xi\sqrt{\frac{\mathfrak{s}_2}{2}}\right]\right), \tag{23}$$

where $\xi = \lambda_1 x + \lambda_2 y + \lambda_3 z + \lambda_4 \dfrac{\Gamma(\omega+1)t^\sigma}{\sigma}$.

In light of result (2.3), Eq. (1) will have the following solutions:

(2.3.1) If $\mathfrak{s}_2 < 0$ and $\mathfrak{s}_4 > 0$, singular soliton form solution is presented as demonstrated:

$$\psi_{2.3.1}(x, y, z, t) = \frac{8\zeta\lambda_1\mathfrak{s}_2}{\beta}\left(\xi + \frac{3}{2\sqrt{-2\mathfrak{s}_2}}\coth\left[2\xi\sqrt{-\frac{\mathfrak{s}_2}{2}}\right]\right), \tag{24}$$

where $\xi = \lambda_1 x + \lambda_2 y + \lambda_3 z + \lambda_4 \dfrac{\Gamma(\omega+1)t^\sigma}{\sigma}$.

(2.3.2) If $\mathfrak{s}_2 > 0$ and $\mathfrak{s}_4 > 0$, singular periodic form solution is presented as demonstrated:

$$\psi_{2.3.2}(x, y, z, t) = \frac{8\zeta\lambda_1\mathfrak{s}_2}{\beta}\left(\xi + \frac{3}{2\sqrt{2\mathfrak{s}_2}}\cot\left[2\xi\sqrt{\frac{\mathfrak{s}_2}{2}}\right]\right), \tag{25}$$

where $\xi = \lambda_1 x + \lambda_2 y + \lambda_3 z + \lambda_4 \dfrac{\Gamma(\omega+1)t^\sigma}{\sigma}$.

Case 3 If $\mathfrak{s}_3 = \mathfrak{s}_4 = \mathfrak{s}_6 = 0$, we get $h_2 = r_1 = 0$, $r_2 = \pm\dfrac{3\zeta\lambda_1\sqrt{\mathfrak{s}_0}}{\beta}$ and

(3.1) $f_0 = 0$, $f_1 = f_2 = 0$, $g_1 = -\dfrac{3\zeta\lambda_1\mathfrak{s}_1}{2\beta}$, $g_2 = -\dfrac{3\zeta\lambda_1\mathfrak{s}_0}{\beta}$, $\lambda_4 = -\dfrac{\gamma\lambda_1^2 + \delta\lambda_3^2 + \zeta\mathfrak{s}_2\lambda_2\lambda_1^3}{\lambda_1+\lambda_2+\lambda_3}$.

(3.2) $f_0 = -\dfrac{\zeta\lambda_1\mathfrak{s}_2}{\beta}$, $f_1 = f_2 = 0$, $g_1 = -\dfrac{3\zeta\lambda_1\mathfrak{s}_1}{2\beta}$, $g_2 = -\dfrac{3\zeta\lambda_1\mathfrak{s}_0}{\beta}$, $\lambda_4 = -\dfrac{\gamma\lambda_1^2 + \delta\lambda_3^2 - \zeta\mathfrak{s}_2\lambda_2\lambda_1^3}{\lambda_1+\lambda_2+\lambda_3}$.

In light of result (3.1), Eq. (1) will have the following solutions:

(3.1.1) If $\mathfrak{s}_2 > 0$, $\mathfrak{s}_0 > 0$ and $\mathfrak{s}_1 = 0$, dark and singular soliton form solutions are presented as demonstrated:

$$\psi_{3.1.1}(x,y,z,t)=\frac{3\zeta\lambda_1\sqrt{\mathfrak{s}_2}}{\beta}\tanh\left[\frac{1}{2}\left(\lambda_1x+\lambda_2y+\lambda_3z+\lambda_4\frac{\Gamma(\omega+1)t^\sigma}{\sigma}\right)\sqrt{\mathfrak{s}_2}\right], \tag{26}$$

or

$$\psi_{3.1.1}(x,y,z,t)=\frac{3\zeta\lambda_1\sqrt{\mathfrak{s}_2}}{\beta}\coth\left[\frac{1}{2}\left(\lambda_1x+\lambda_2y+\lambda_3z+\lambda_4\frac{\Gamma(\omega+1)t^\sigma}{\sigma}\right)\sqrt{\mathfrak{s}_2}\right]. \tag{27}$$

(3.1.2) If $\mathfrak{s}_2<0$, $\mathfrak{s}_0>0$ and $\mathfrak{s}_1=0$, singular periodic form solutions are presented as demonstrated:

$$\psi_{3.1.2}(x,y,z,t)=\frac{3\zeta\lambda_1\sqrt{-\mathfrak{s}_2}}{\beta}\tan\left[\frac{1}{2}\left(\lambda_1x+\lambda_2y+\lambda_3z+\lambda_4\frac{\Gamma(\omega+1)t^\sigma}{\sigma}\right)\sqrt{-\mathfrak{s}_2}\right], \tag{28}$$

or

$$\psi_{3.1.2}(x,y,z,t)=\frac{3\zeta\lambda_1\sqrt{-\mathfrak{s}_2}}{\beta}\cot\left[\frac{1}{2}\left(\lambda_1x+\lambda_2y+\lambda_3z+\lambda_4\frac{\Gamma(\omega+1)t^\sigma}{\sigma}\right)\sqrt{-\mathfrak{s}_2}\right]. \tag{29}$$

(3.1.3) If $\mathfrak{s}_2>0$ and $\mathfrak{s}_0=\frac{\mathfrak{s}_1^2}{4\mathfrak{s}_2}$, an exponential solution is presented as demonstrated:

$$\psi_{3.1.2}(x,y,z,t)=\frac{6\zeta\lambda_1\sqrt{\mathfrak{s}_2}}{\beta}\left(\frac{\mathfrak{s}_1}{\mathfrak{s}_1-2\mathfrak{s}_2e^{\left(\lambda_1x+\lambda_2y+\lambda_3z+\lambda_4\frac{\Gamma(\omega+1)t^\sigma}{\sigma}\right)\sqrt{\mathfrak{s}_2}}}\right), \tag{30}$$

where $\mathfrak{s}_1-2\mathfrak{s}_2e^{\left(\lambda_1x+\lambda_2y+\lambda_3z+\lambda_4\frac{\Gamma(\omega+1)t^\sigma}{\sigma}\right)\sqrt{\mathfrak{s}_2}}\neq 0$.

In light of result (3.2), Eq. (1) will have the following solutions:

(3.2.1) If $\mathfrak{s}_2>0$, $\mathfrak{s}_0>0$ and $\mathfrak{s}_1=0$, dark and singular soliton form solutions are presented as demonstrated:

$$\psi_{3.2.1}(x,y,z,t)=-\frac{\zeta\lambda_1\mathfrak{s}_2}{\beta}\left(\xi+\frac{3}{\sqrt{\mathfrak{s}_2}}\tanh\left[\frac{1}{2}\xi\sqrt{\mathfrak{s}_2}\right]\right), \tag{31}$$

or

$$\psi_{3.2.1}(x,y,z,t)=-\frac{\zeta\lambda_1\mathfrak{s}_2}{\beta}\left(\xi+\frac{3}{\sqrt{\mathfrak{s}_2}}\coth\left[\frac{1}{2}\xi\sqrt{\mathfrak{s}_2}\right]\right), \tag{32}$$

where $\xi=\lambda_1x+\lambda_2y+\lambda_3z+\lambda_4\frac{\Gamma(\omega+1)t^\sigma}{\sigma}$.

(3.2.2) If $\mathfrak{s}_2<0$, $\mathfrak{s}_0>0$ and $\mathfrak{s}_1=0$, singular periodic form solutions are presented as demonstrated:

$$\psi_{3.2.2}(x,y,z,t) = -\frac{\zeta\lambda_1\mathfrak{s}_2}{\beta}\left(\xi + \frac{3}{\sqrt{-\mathfrak{s}_2}}\tan\left[\xi\sqrt{-\mathfrak{s}_2}\right]\right), \tag{33}$$

or

$$\psi_{3.2.2}(x,y,z,t) = -\frac{\zeta\lambda_1\mathfrak{s}_2}{\beta}\left(\xi + \frac{3}{\sqrt{-\mathfrak{s}_2}}\cot\left[\frac{1}{2}\xi\sqrt{-\mathfrak{s}_2}\right]\right), \tag{34}$$

where $\xi = \lambda_1 x + \lambda_2 y + \lambda_3 z + \lambda_4 \dfrac{\Gamma(\omega+1)t^\sigma}{\sigma}$.

(3.2.3) If $\mathfrak{s}_2 > 0$ and $\mathfrak{s}_0 = \dfrac{\mathfrak{s}_1^2}{4\mathfrak{s}_2}$, an exponential solution is presented as demonstrated:

$$\psi_{3.2.3}(x,y,z,t) = -\frac{\zeta\lambda_1\sqrt{\mathfrak{s}_2}}{\beta}\left(\xi\sqrt{\mathfrak{s}_2} + \frac{6\mathfrak{s}_1}{\mathfrak{s}_1 - 2\mathfrak{s}_2 e^{\xi\sqrt{\mathfrak{s}_2}}}\right), \tag{35}$$

where $\xi = \lambda_1 x + \lambda_2 y + \lambda_3 z + \lambda_4 \dfrac{\Gamma(\omega+1)t^\sigma}{\sigma}$ and $\mathfrak{s}_1 - 2\mathfrak{s}_2 e^{\left(\lambda_1 x+\lambda_2 y+\lambda_3 z+\lambda_4\frac{\Gamma(\omega+1)t^\sigma}{\sigma}\right)\sqrt{\mathfrak{s}_2}} \neq 0$.

Case 4 If $\mathfrak{s}_0 = \mathfrak{s}_1 = \mathfrak{s}_6 = 0$, we get $h_2 = r_1 = r_2 = 0$ and

(4.1) $f_0 = 0$, $f_1 = 0$, $f_2 = -\dfrac{(5\mathfrak{s}_3 + 6\mathfrak{s}_4)\,\zeta\lambda_1}{\beta}$, $g_1 = 0$, $g_2 = 0$, $\lambda_4 = -\dfrac{\gamma\lambda_1^2 + \delta\lambda_3^2 + 4\zeta\mathfrak{s}_2\lambda_2\lambda_1^3}{\lambda_1+\lambda_2+\lambda_3}$.

(4.2) $f_0 = -\dfrac{4\zeta\lambda_1\mathfrak{s}_2}{\beta}$, $f_1 = 0$, $f_2 = -\dfrac{(5\mathfrak{s}_3 + 6\mathfrak{s}_4)\,\zeta\lambda_1}{\beta}$, $g_1 = 0$, $g_2 = 0$, $\lambda_4 = -\dfrac{\gamma\lambda_1^2 + \delta\lambda_3^2 - 4\zeta\mathfrak{s}_2\lambda_2\lambda_1^3}{\lambda_1+\lambda_2+\lambda_3}$.

In light of result (4.1), Eq. (1) will have the following solutions:

(4.1.1) If $\mathfrak{s}_2 > 0$ and $\mathfrak{s}_3^2 = 4\mathfrak{s}_2\mathfrak{s}_4$, dark soliton form solution is presented as demonstrated:

$$\psi_{4.1.1}(x,y,z,t) = -\frac{\zeta\lambda_1\,(5\mathfrak{s}_2 + 3\sqrt{\mathfrak{s}_2\mathfrak{s}_4})}{\beta\sqrt{\mathfrak{s}_4}}\left(-2\mathrm{Log}\left|1 - \tanh\left[\frac{\xi\sqrt{\mathfrak{s}_2}}{2}\right]\right| - \tanh\left[\frac{\xi\sqrt{\mathfrak{s}_2}}{2}\right]\right), \tag{36}$$

where $\xi = \lambda_1 x + \lambda_2 y + \lambda_3 z + \lambda_4 \dfrac{\Gamma(\omega+1)t^\sigma}{\sigma}$.

(4.1.2) If $\mathfrak{s}_2 > 0$ and $\mathfrak{s}_3^2 = 4\mathfrak{s}_2\mathfrak{s}_4$, hyperbolic form solution is presented as demonstrated:

$$\psi_{4.1.2}(x,y,z,t) = -\frac{\zeta\lambda_1\,(5\mathfrak{s}_2 + 3\sqrt{\mathfrak{s}_2\mathfrak{s}_4})}{\beta\sqrt{\mathfrak{s}_4}}\left(\xi\sqrt{\mathfrak{s}_2} + 2\mathrm{Log}\left|\sinh\left[\frac{\xi\sqrt{\mathfrak{s}_2}}{2}\right]\right| - \coth\left[\frac{\xi\sqrt{\mathfrak{s}_2}}{2}\right]\right), \tag{37}$$

where $\xi = \lambda_1 x + \lambda_2 y + \lambda_3 z + \lambda_4 \dfrac{\Gamma(\omega+1)t^\sigma}{\sigma}$.

In light of result (4.2), Eq. (1) will have the following solutions:

(4.2.1) If $\mathfrak{s}_2 > 0$ and $\mathfrak{s}_3^2 = 4\mathfrak{s}_2\mathfrak{s}_4$, dark soliton form solution is presented as demonstrated:

$$\psi_{4.2.1}(x,y,z,t) = -\frac{4\zeta\lambda_1}{\beta}\left(\mathfrak{s}_2\xi + \frac{\zeta\lambda_1\,(5\mathfrak{s}_2 + 3\sqrt{\mathfrak{s}_2\mathfrak{s}_4})}{\beta\sqrt{\mathfrak{s}_4}}\left(-2\mathrm{Log}\left|1 - \tanh\left[\frac{\xi\sqrt{\mathfrak{s}_2}}{2}\right]\right| - \tanh\left[\frac{\xi\sqrt{\mathfrak{s}_2}}{2}\right]\right)\right), \tag{38}$$

where $\xi = \lambda_1 x + \lambda_2 y + \lambda_3 z + \lambda_4 \dfrac{\Gamma(\omega+1)t^{\sigma}}{\sigma}$.

(4.2.2) If $\mathfrak{s}_2 > 0$ and $\mathfrak{s}_3^2 = 4\mathfrak{s}_2\mathfrak{s}_4$, hyperbolic form solution is presented as demonstrated:

$$\psi_{4.2.2}(x,y,z,t) = -\frac{4\zeta\lambda_1}{\beta}\left(\xi - \frac{\zeta\lambda_1\left(5\mathfrak{s}_2 + 3\sqrt{\mathfrak{s}_2\mathfrak{s}_4}\right)}{\beta\sqrt{\mathfrak{s}_4}}\left(\xi\sqrt{\mathfrak{s}_2} + 2\mathrm{Log}\left|\sinh\left[\frac{\xi\sqrt{\mathfrak{s}_2}}{2}\right]\right| - \coth\left[\frac{\xi\sqrt{\mathfrak{s}_2}}{2}\right]\right)\right), \tag{39}$$

where $\xi = \lambda_1 x + \lambda_2 y + \lambda_3 z + \lambda_4 \dfrac{\Gamma(\omega+1)t^{\sigma}}{\sigma}$.

Case 5 If $\mathfrak{s}_1 = \mathfrak{s}_3 = 0$, we get $f_2 = h_2 = r_1 = r_2 = 0$ and

(5.1) $f_0 = -\dfrac{2\zeta\lambda_1\left(\mathfrak{s}_2 \pm \sqrt{\mathfrak{s}_2^2 - 3\mathfrak{s}_0\mathfrak{s}_4}\right)}{\beta}$, $f_1 = 0$, $g_1 = 0$, $g_2 = -\dfrac{6\zeta\lambda_1\mathfrak{s}_0}{\beta}$, $\lambda_4 = -\dfrac{\delta\lambda_3^2 + \gamma\lambda_1^2 \pm 4\zeta\lambda_1^3\lambda_2\sqrt{\mathfrak{s}_2^2 - 3\mathfrak{s}_0\mathfrak{s}_4}}{\lambda_1+\lambda_2+\lambda_3}$.

In light of result (5.1), Eq. (1) will have the following solutions:

(5.1.1) If $\mathfrak{s}_2 > 0$, hyperbolic form solutions are presented as demonstrated:

$$\psi_{5.1.1}(x,y,z,t) = \frac{\zeta\lambda_1}{\beta\mathfrak{s}_2}\left(\left(3\mathfrak{s}_0\mathfrak{s}_4 - 2\mathfrak{s}_2^2 \pm 2\mathfrak{s}_2\sqrt{\mathfrak{s}_2^2 - 3\mathfrak{s}_0\mathfrak{s}_4}\right)\xi - \frac{3\mathfrak{s}_0\sqrt{\mathfrak{s}_4^2 - 4\mathfrak{s}_2\mathfrak{s}_6}}{2\sqrt{\mathfrak{s}_2}}\sinh\left[2\xi\sqrt{\mathfrak{s}_2}\right]\right), \tag{40}$$

where $\xi = \lambda_1 x + \lambda_2 y + \lambda_3 z + \lambda_4 \dfrac{\Gamma(\omega+1)t^{\sigma}}{\sigma}$.

(5.1.2) If $\mathfrak{s}_2 < 0$, a periodic form solutions are presented as demonstrated:

$$\psi_{5.1.2}(x,y,z,t) = \frac{\zeta\lambda_1}{\beta\mathfrak{s}_2}\left(\left(3\mathfrak{s}_0\mathfrak{s}_4 - 2\mathfrak{s}_2^2 \pm 2\mathfrak{s}_2\sqrt{\mathfrak{s}_2^2 - 3\mathfrak{s}_0\mathfrak{s}_4}\right)\xi - \frac{3\mathfrak{s}_0\sqrt{\mathfrak{s}_4^2 - 4\mathfrak{s}_2\mathfrak{s}_6}}{2\sqrt{-\mathfrak{s}_2}}\sin\left[2\xi\sqrt{-\mathfrak{s}_2}\right]\right), \tag{41}$$

where $\xi = \lambda_1 x + \lambda_2 y + \lambda_3 z + \lambda_4 \dfrac{\Gamma(\omega+1)t^{\sigma}}{\sigma}$.

Case 6 If $\mathfrak{s}_1 = \mathfrak{s}_3 = \mathfrak{s}_6 = 0$, we get $f_1 = g_1 = h_2 = r_1 = r_2 = 0$ and

(6.1) $f_0 = -\dfrac{2\zeta\lambda_1\left(\mathfrak{s}_2 \pm \sqrt{\mathfrak{s}_2^2 - 3\mathfrak{s}_0\mathfrak{s}_4}\right)}{\beta}$, $f_2 = 0$, $g_2 = -\dfrac{6\zeta\lambda_1\mathfrak{s}_0}{\beta}$, $\lambda_4 = -\dfrac{\delta\lambda_3^2 + \gamma\lambda_1^2 \mp 4\zeta\lambda_1^3\lambda_2\sqrt{\mathfrak{s}_2^2 - 3\mathfrak{s}_0\mathfrak{s}_4}}{\lambda_1+\lambda_2+\lambda_3}$.

(6.2) $f_0 = -\dfrac{2\zeta\lambda_1\left(\mathfrak{s}_2 \pm \sqrt{\mathfrak{s}_2^2 - 3\mathfrak{s}_0\mathfrak{s}_4}\right)}{\beta}$, $f_2 = -\dfrac{6\zeta\lambda_1\mathfrak{s}_4}{\beta}$, $g_2 = 0$, $\lambda_4 = -\dfrac{\delta\lambda_3^2 + \gamma\lambda_1^2 \mp 4\zeta\lambda_1^3\lambda_2\sqrt{\mathfrak{s}_2^2 - 3\mathfrak{s}_0\mathfrak{s}_4}}{\lambda_1+\lambda_2+\lambda_3}$.

(6.3) $f_0 = -\dfrac{2\zeta\lambda_1\left(\mathfrak{s}_2 \pm \sqrt{\mathfrak{s}_2^2 + 12\mathfrak{s}_0\mathfrak{s}_4}\right)}{\beta}$, $f_2 = -\dfrac{6\zeta\lambda_1\mathfrak{s}_4}{\beta}$, $g_2 = -\dfrac{6\zeta\lambda_1\mathfrak{s}_0}{\beta}$, $\lambda_4 = -\dfrac{\left(\begin{array}{c}\delta\lambda_3^2 + \gamma\lambda_1^2 \\ \mp 4\zeta\lambda_1^3\lambda_2\sqrt{\mathfrak{s}_2^2 + 12\mathfrak{s}_0\mathfrak{s}_4}\end{array}\right)}{\lambda_1+\lambda_2+\lambda_3}$.

In light of result (6.1), Eq. (1) will have the following solutions:

(6.1.1) If $\mathfrak{s}_0 = 1$, $\mathfrak{s}_2 = -\mathfrak{m}^2 - 1$ and $\mathfrak{s}_4 = \mathfrak{m}^2$, Jacobi elliptic function form solution is presented as demonstrated:

$$\psi_{6.1.1}(x,y,z,t) = -\frac{2\zeta\lambda_1}{\beta}\left(\left(2 - \mathfrak{m}^2 + \sqrt{\mathfrak{m}^4 - \mathfrak{m}^2 + 1}\right)\xi - 3\varepsilon[\xi] - 3\frac{\mathrm{cn}[\xi]\mathrm{dn}[\xi]}{\mathrm{sn}[\xi]}\right), \tag{42}$$

or

$$\psi_{6.1.1}(x,y,z,t) = -\frac{2\zeta\lambda_1}{\beta}\left(\left(2-\mathfrak{m}^2+\sqrt{\mathfrak{m}^4-\mathfrak{m}^2+1}\right)\xi - 3\varepsilon[\xi]+3\mathrm{dn}[\xi]\mathrm{sc}[\xi]\right), \tag{43}$$

where $\xi = \lambda_1 x+\lambda_2 y+\lambda_3 z+\lambda_4\dfrac{\Gamma(\omega+1)t^\sigma}{\sigma}$ and $0\le\mathfrak{m}\le 1$.

When putting $\mathfrak{m}=1$ in Eq. (40), a singular soliton form solution is presented as demonstrated:

$$\psi_{6.1.1.1}(x,y,z,t) = \frac{4\zeta\lambda_1}{\beta}\left(\lambda_1 x+\lambda_2 y+\lambda_3 z+\lambda_4\frac{\Gamma(\omega+1)t^\sigma}{\sigma}+\frac{3}{2}\coth\left[\lambda_1 x+\lambda_2 y+\lambda_3 z+\lambda_4\frac{\Gamma(\omega+1)t^\sigma}{\sigma}\right]\right). \tag{44}$$

When putting $\mathfrak{m}=0$ in Eq. (40) and Eq. (41) respectively, singular periodic form solutions are presented as demonstrated:

$$\psi_{6.1.1.2}(x,y,z,t) = \frac{4\zeta\lambda_1}{\beta}\left(\lambda_1 x+\lambda_2 y+\lambda_3 z+\lambda_4\frac{\Gamma(\omega+1)t^\sigma}{\sigma}+\frac{3}{2}\cot\left[\lambda_1 x+\lambda_2 y+\lambda_3 z+\lambda_4\frac{\Gamma(\omega+1)t^\sigma}{\sigma}\right]\right), \tag{45}$$

and

$$\psi_{6.1.1.2}(x,y,z,t) = \frac{4\zeta\lambda_1}{\beta}\left(\lambda_1 x+\lambda_2 y+\lambda_3 z+\lambda_4\frac{\Gamma(\omega+1)t^\sigma}{\sigma}-\frac{3}{2}\tan\left[\lambda_1 x+\lambda_2 y+\lambda_3 z+\lambda_4\frac{\Gamma(\omega+1)t^\sigma}{\sigma}\right]\right). \tag{46}$$

(6.1.2) If $\mathfrak{s}_0=\mathfrak{m}^2-1$, $\mathfrak{s}_2=2-\mathfrak{m}^2$ and $\mathfrak{s}_4=-1$, a Jacobi elliptic function form solution is presented as demonstrated:

$$\psi_{6.1.2}(x,y,z,t) = -\frac{2\zeta\lambda_1}{\beta}\left(\left(2-\mathfrak{m}^2+\sqrt{\mathfrak{m}^4-\mathfrak{m}^2+1}\right)\xi - 3(\mathfrak{m}+1)\varepsilon[\xi]+3\frac{\mathfrak{m}(\mathfrak{m}+1)\mathrm{cn}[\xi]\mathrm{sn}[\xi]}{\mathrm{dn}[\xi]}\right), \tag{47}$$

where $\xi = \lambda_1 x+\lambda_2 y+\lambda_3 z+\lambda_4\dfrac{\Gamma(\omega+1)t^\sigma}{\sigma}$ and $0\le\mathfrak{m}\le 1$.

(6.1.3) If $\mathfrak{s}_0=-\mathfrak{m}^2$, $\mathfrak{s}_2=-1+2\mathfrak{m}^2$ and $\mathfrak{s}_4=1-\mathfrak{m}^2$, a Jacobi elliptic function form solution is presented as demonstrated:

$$\psi_{6.1.3}(x,y,z,t) = -\frac{2\zeta\lambda_1}{\beta}\left(\left(-\mathfrak{m}^2+3\mathfrak{m}-1+\sqrt{\mathfrak{m}^4-\mathfrak{m}^2+1}\right)\xi - 3\mathfrak{m}\varepsilon[\xi]\right), \tag{48}$$

where $\xi = \lambda_1 x+\lambda_2 y+\lambda_3 z+\lambda_4\dfrac{\Gamma(\omega+1)t^\sigma}{\sigma}$ and $0\le\mathfrak{m}\le 1$.

When putting $\mathfrak{m}=1$ in Eq. (48), a dark soliton form solution is presented as demonstrated:

$$\psi_{6.1.3.1}(x,y,z,t) = -\frac{4\zeta\lambda_1}{\beta}\left(\lambda_1 x+\lambda_2 y+\lambda_3 z+\lambda_4\frac{\Gamma(\omega+1)t^\sigma}{\sigma}-\frac{3}{2}\tanh\left[\lambda_1 x+\lambda_2 y+\lambda_3 z+\lambda_4\frac{\Gamma(\omega+1)t^\sigma}{\sigma}\right]\right). \tag{49}$$

(6.1.4) If $\mathfrak{s}_0=-1$, $\mathfrak{s}_2=2-\mathfrak{m}^2$ and $\mathfrak{s}_4=\mathfrak{m}^2-1$, a Jacobi elliptic function form solution is presented as demonstrated:

$$\psi_{6.1.4}(x,y,z,t) = -\frac{2\zeta\lambda_1}{\beta}\left(\left(2-\mathfrak{m}^2+\sqrt{\mathfrak{m}^4-\mathfrak{m}^2+1}\right)\xi - 3\varepsilon[\xi]\right), \tag{50}$$

where $\xi = \lambda_1 x+\lambda_2 y+\lambda_3 z+\lambda_4\dfrac{\Gamma(\omega+1)t^\sigma}{\sigma}$ and $0\le\mathfrak{m}\le 1$.

(6.1.5) If $\mathfrak{s}_0=\dfrac{1}{4}$, $\mathfrak{s}_2=\dfrac{1}{2}(\mathfrak{m}^2-2)$ and $\mathfrak{s}_4=\dfrac{\mathfrak{m}^4}{4}$, a Jacobi elliptic function form solution is presented as demonstrated:

$$\psi_{6.1.5}(x,y,z,t) = \frac{\zeta\lambda_1}{2\beta}\left(\left(-2\mathfrak{m}^2+3\mathfrak{m}-2+\sqrt{\mathfrak{m}^4-16\mathfrak{m}^2+16}\right)\xi + 6\varepsilon[\xi] + \frac{6\mathrm{cn}[\xi](\mathrm{dn}[\xi]+1)}{\mathrm{sn}[\xi]}\right), \tag{51}$$

where $\xi = \lambda_1 x+\lambda_2 y+\lambda_3 z+\lambda_4\dfrac{\Gamma(\omega+1)t^\sigma}{\sigma}$ and $0\le\mathfrak{m}\le 1$.

When putting $\mathfrak{m}=1$ in Eq. (51), a singular soliton form solution is presented as demonstrated:

$$\begin{aligned}&\psi_{6.1.5.1}(x,y,z,t)\\ &= -\frac{\zeta\lambda_1}{\beta}\left(\lambda_1 x+\lambda_2 y+\lambda_3 z+\lambda_4\frac{\Gamma(\omega+1)t^\sigma}{\sigma} - 3\coth\left[\frac{1}{2}\left(\lambda_1 x+\lambda_2 y+\lambda_3 z+\lambda_4\frac{\Gamma(\omega+1)t^\sigma}{\sigma}\right)\right]\right).\end{aligned} \tag{52}$$

In light of result (6.2), Eq. (1) will have the following solutions:

(6.2.1) If $\mathfrak{s}_0=1$, $\mathfrak{s}_2=-\mathfrak{m}^2-1$ and $\mathfrak{s}_4=\mathfrak{m}^2$, a Jacobi elliptic function form solution is presented as demonstrated:

$$\psi_{6.2.1}(x,y,z,t) = -\frac{2\zeta\lambda_1}{\beta}\left(\left(-1-\mathfrak{m}^2+3\mathfrak{m}\pm\sqrt{\mathfrak{m}^4-\mathfrak{m}^2+1}\right)\xi - 3\varepsilon[\xi]\right), \tag{53}$$

or

$$\psi_{6.2.1}(x,y,z,t) = -\frac{2\zeta\lambda_1}{\beta}\left(\left(-1-\mathfrak{m}^2+3\mathfrak{m}+\sqrt{\mathfrak{m}^4-\mathfrak{m}^2+1}\right)\xi - 3\varepsilon[\xi] + 3\mathfrak{m}^2\frac{\mathrm{cn}[\xi]\mathrm{sn}[\xi]}{\mathrm{dn}[\xi]}\right), \tag{54}$$

where $\xi = \lambda_1 x+\lambda_2 y+\lambda_3 z+\lambda_4\dfrac{\Gamma(\omega+1)t^\sigma}{\sigma}$ and $0\le\mathfrak{m}\le 1$.

(6.2.2) If $\mathfrak{s}_0=\mathfrak{m}^2-1$, $\mathfrak{s}_2=2-\mathfrak{m}^2$ and $\mathfrak{s}_4=-1$, a Jacobi elliptic function form solution is presented as demonstrated:

$$\psi_{6.2.2}(x,y,z,t) = -\frac{2\zeta\lambda_1}{\beta}\left(\left(-1-\mathfrak{m}^2+\sqrt{\mathfrak{m}^4-\mathfrak{m}^2+1}\right)\xi + 3\mathfrak{m}^2\varepsilon[\xi]\right), \tag{55}$$

where $\xi = \lambda_1 x+\lambda_2 y+\lambda_3 z+\lambda_4\dfrac{\Gamma(\omega+1)t^\sigma}{\sigma}$ and $0\le\mathfrak{m}\le 1$.

When putting $\mathfrak{m}=1$ in Eq. (55), a dark soliton form solution is presented as demonstrated:

$$\psi_{6.2.2.1}(x,y,z,t)=\frac{2\zeta\lambda_1}{\beta}\left(\lambda_1x+\lambda_2y+\lambda_3z+\lambda_4\frac{\Gamma(\omega+1)t^{\sigma}}{\sigma}-3\tanh\left[\lambda_1x+\lambda_2y+\lambda_3z+\lambda_4\frac{\Gamma(\omega+1)t^{\sigma}}{\sigma}\right]\right). \quad (56)$$

(6.2.3) If $\mathfrak{s}_0=-\mathfrak{m}^2$, $\mathfrak{s}_2=-1+2\mathfrak{m}^2$ and $\mathfrak{s}_4=1-\mathfrak{m}^2$, a Jacobi elliptic function form solution is presented as demonstrated:

$$\psi_{6.2.3}(x,y,z,t)=\frac{2\zeta\lambda_1}{\beta}\left[\left(1-2\mathfrak{m}^2-\sqrt{\mathfrak{m}^4-\mathfrak{m}^2+1}\right)\xi-\frac{3\mathfrak{m}^2}{\mathfrak{m}-1}\left(\varepsilon[\xi]-\frac{\mathrm{dn}[\xi]\mathrm{sn}[\xi]}{\mathrm{cn}[\xi]}\right)\right], \quad (57)$$

where $\xi=\lambda_1x+\lambda_2y+\lambda_3z+\lambda_4\dfrac{\Gamma(\omega+1)t^{\sigma}}{\sigma}$ and $0\le\mathfrak{m}<1$.

(6.2.4) If $\mathfrak{s}_0=-1$, $\mathfrak{s}_2=2-\mathfrak{m}^2$ and $\mathfrak{s}_4=\mathfrak{m}^2-1$, a Jacobi elliptic function form solution is presented as demonstrated:

$$\psi_{6.2.4}(x,y,z,t)=-\frac{2\zeta\lambda_1}{\beta}\left[\left(2-\mathfrak{m}^2+\sqrt{\mathfrak{m}^4-\mathfrak{m}^2+1}\right)\xi-3(\mathfrak{m}+1)\left(\varepsilon[\xi]-\frac{3\mathfrak{m}\mathrm{cn}[\xi]\mathrm{sn}[\xi]}{\mathrm{dn}[\xi]}\right)\right], \quad (58)$$

where $\xi=\lambda_1x+\lambda_2y+\lambda_3z+\lambda_4\dfrac{\Gamma(\omega+1)t^{\sigma}}{\sigma}$ and $0\le\mathfrak{m}\le1$.

When putting $\mathfrak{m}=1$ in Eq. (58), a dark soliton form solution is presented as demonstrated:

$$\psi_{6.2.4.1}(x,y,z,t)=-\frac{4\zeta\lambda_1}{\beta}\left(\lambda_1x+\lambda_2y+\lambda_3z+\lambda_4\frac{\Gamma(\omega+1)t^{\sigma}}{\sigma}+6\tanh\left[\lambda_1x+\lambda_2y+\lambda_3z+\lambda_4\frac{\Gamma(\omega+1)t^{\sigma}}{\sigma}\right]\right), \quad (59)$$

(6.2.5) If $\mathfrak{s}_0=\dfrac{1}{4}$, $\mathfrak{s}_2=\dfrac{1}{2}(\mathfrak{m}^2-2)$ and $\mathfrak{s}_4=\dfrac{\mathfrak{m}^4}{4}$, a Jacobi elliptic function form solution is presented as demonstrated:

$$\psi_{6.2.5}(x,y,z,t)=-\frac{\zeta\lambda_1}{2\beta}\left(\left(-4+8\mathfrak{m}^2-3\mathfrak{m}^3\pm\sqrt{\mathfrak{m}^4-16\mathfrak{m}^2+16}\right)\xi-6\mathfrak{m}^2\varepsilon[\xi]-\frac{6m^2(\mathrm{dn}[\xi]-1)}{\mathrm{sc}[\xi]}\right), \quad (60)$$

where $\xi=\lambda_1x+\lambda_2y+\lambda_3z+\lambda_4\dfrac{\Gamma(\omega+1)t^{\sigma}}{\sigma}$ and $0\le\mathfrak{m}\le1$.

In light of result (6.3), Eq. (1) will have the following solutions:

(6.3.1) If $\mathfrak{s}_0=1$, $\mathfrak{s}_2=-\mathfrak{m}^2-1$ and $\mathfrak{s}_4=\mathfrak{m}^2$, a Jacobi elliptic function form solution is presented as demonstrated:

$$\psi_{6.3.1}(x,y,z,t)=-\frac{2\zeta\lambda_1}{\beta}\left(\left(2-\mathfrak{m}^2+3\mathfrak{m}+\sqrt{\mathfrak{m}^4+14\mathfrak{m}^2+1}\right)\xi-3(\mathfrak{m}+1)\varepsilon[\xi]-3\frac{\mathrm{cn}[\xi]\mathrm{dn}[\xi]}{\mathrm{sn}[\xi]}\right), \quad (61)$$

where $\xi=\lambda_1x+\lambda_2y+\lambda_3z+\lambda_4\dfrac{\Gamma(\omega+1)t^{\sigma}}{\sigma}$ and $0\le\mathfrak{m}\le1$.

When putting $\mathfrak{m}=1$ in Eq. (61), a singular soliton form solution is presented as demonstrated:

$$\psi_{6.3.1.1}(x, y, z, t)$$

$$= -\frac{8\zeta\lambda_1}{\beta}\left(\lambda_1 x+\lambda_2 y+\lambda_3 z+\lambda_4\frac{\Gamma(\omega+1)t^{\sigma}}{\sigma}-\frac{3}{4}\coth\left[2\left(\lambda_1 x+\lambda_2 y+\lambda_3 z+\lambda_4\frac{\Gamma(\omega+1)t^{\sigma}}{\sigma}\right)\right]\right), \tag{62}$$

where $\xi=\lambda_1 x+\lambda_2 y+\lambda_3 z+\lambda_4\dfrac{\Gamma(\omega+1)t^{\sigma}}{\sigma}$.

(6.3.2) If $\mathfrak{s}_0=\mathfrak{m}^2-1$, $\mathfrak{s}_2=2-\mathfrak{m}^2$ and $\mathfrak{s}_4=-1$, a Jacobi elliptic function form solution is presented as demonstrated:

$$\psi_{6.3.2}(x, y, z, t)$$

$$= -\frac{2\zeta\lambda_1}{\beta}\left(\left(-1-\mathfrak{m}^2+\sqrt{\mathfrak{m}^4+14\mathfrak{m}^2+1}\right)\xi-\frac{3}{\mathfrak{m}-1}\left((-\mathfrak{m}^3+\mathfrak{m}^2+1)\varepsilon[\xi]-3\mathfrak{m}\frac{\mathrm{cn}[\xi]\mathrm{sn}[\xi]}{\mathrm{dn}[\xi]}\right)\right), \tag{63}$$

where $\xi=\lambda_1 x+\lambda_2 y+\lambda_3 z+\lambda_4\dfrac{\Gamma(\omega+1)t^{\sigma}}{\sigma}$ and $0\le\mathfrak{m}<1$.

(6.3.3) If $\mathfrak{s}_0=-\mathfrak{m}^2$, $\mathfrak{s}_2=-1+2\mathfrak{m}^2$ and $\mathfrak{s}_4=1-\mathfrak{m}^2$, a Jacobi elliptic function form solution is presented as demonstrated:

$$\psi_{6.3.3}(x, y, z, t)$$

$$= -\frac{2\zeta\lambda_1}{\mathfrak{m}\beta}\left[\left(-3+2\mathfrak{m}^3+2\mathfrak{m}+\sqrt{\mathfrak{m}^4+14\mathfrak{m}^2+1}\right)\xi+\frac{3}{m-1}\left((-m^3+m-1)\varepsilon[\xi]-3m\frac{\mathrm{dn}[\xi]\mathrm{sn}[\xi]}{\mathrm{cn}[\xi]}\right)\right], \tag{64}$$

where $\xi=\lambda_1 x+\lambda_2 y+\lambda_3 z+\lambda_4\dfrac{\Gamma(\omega+1)t^{\sigma}}{\sigma}$ and $0<\mathfrak{m}<1$.

(6.3.4) If $\mathfrak{s}_0=-1$, $\mathfrak{s}_2=2-\mathfrak{m}^2$ and $\mathfrak{s}_4=\mathfrak{m}^2-1$, a Jacobi elliptic function form solution is presented as demonstrated:

$$\psi_{6.3.4}(x, y, z, t)=-\frac{2\zeta\lambda_1}{\beta}\left(\left(2-\mathfrak{m}^2\pm\sqrt{\mathfrak{m}^4-16\mathfrak{m}^2+16}\right)\xi-3(\mathfrak{m}+2)\varepsilon[\xi]+3\mathfrak{m}(\mathfrak{m}+1)\frac{\mathrm{cn}[\xi]\mathrm{sn}[\xi]}{\mathrm{dn}[\xi]}\right), \tag{65}$$

where $\xi=\lambda_1 x+\lambda_2 y+\lambda_3 z+\lambda_4\dfrac{\Gamma(\omega+1)t^{\sigma}}{\sigma}$ and $0\le\mathfrak{m}\le1$.

(6.3.5) If $\mathfrak{s}_0=\dfrac{1}{4}$, $\mathfrak{s}_2=\dfrac{1}{2}(\mathfrak{m}^2-2)$ and $\mathfrak{s}_4=\dfrac{\mathfrak{m}^4}{4}$, a Jacobi elliptic function form solution is presented as demonstrated:

$$\psi_{6.3.5}(x, y, z, t)=-\frac{2\zeta\lambda_1}{\mathfrak{m}^2\beta}\left(\left(-\mathfrak{m}^4+2\mathfrak{m}^2+3\mathfrak{m}-6+\mathfrak{m}^2\sqrt{\mathfrak{m}^4-16\mathfrak{m}^2+16}\right)\xi+6\varepsilon[\xi]+6\frac{2m^2-1+\mathrm{dn}[\xi]}{\mathrm{sc}[\xi]}\right), \tag{66}$$

where $\xi=\lambda_1 x+\lambda_2 y+\lambda_3 z+\lambda_4\dfrac{\Gamma(\omega+1)t^{\sigma}}{\sigma}$ and $0<\mathfrak{m}\le1$.

When putting $\mathfrak{m}=1$ in Eq. (66), a singular soliton form solutions is presented as demonstrated:

$$\psi_{6.3.5.1}(x, y, z, t)$$

$$= \frac{2\zeta\lambda_1}{\beta}\left(\lambda_1 x+\lambda_2 y+\lambda_3 z+\lambda_4\frac{\Gamma(\omega+1)t^{\sigma}}{\sigma}-6\coth\left[\frac{1}{2}\left(\lambda_1 x+\lambda_2 y+\lambda_3 z+\lambda_4\frac{\Gamma(\omega+1)t^{\sigma}}{\sigma}\right)\right]\right). \tag{67}$$

4. Stability analysis of the fractional PDE

Understanding the stability characteristics of nonlinear Partial Differential Equations (PDEs) is crucial for predicting the long-term behavior of dynamical systems across various scientific domains. This section presents a rigorous linear stability analysis of the proposed fractional-order PDE, which incorporates mixed partial derivatives and nonlinear coupling terms. To analyze the stability of Eq. (1), we employ linear stability analysis by examining small perturbations around a steady-state solution. Assume a solution of the form:

$$V = \mathscr{H}(x, t)+\mathscr{A}, \tag{68}$$

where $\mathscr{A}$ represents a small perturbation.

Substituting (68) into (1) yields the linearized equation:

$$D_{M,t}^{\sigma,\mu}\left(\mathscr{H}_x+\mathscr{H}_y+\mathscr{H}_z\right)+\zeta\mathscr{H}_{xxxy}+\gamma\mathscr{H}_{xx}+\delta\mathscr{H}_{zz}=0. \tag{69}$$

We consider solutions of the form:

$$\mathscr{H} = \Psi e^{i(k_1x+k_2y+k_3z)+\varpi t}, \tag{70}$$

where Ψ is a small amplitude, k_i (for $i = 1, 2, 3$) are wavenumbers in the x, y, and z directions respectively, and ϖ is the growth rate.

The growth rate ϖ is given by:

$$\varpi = -\frac{i\Gamma(\mu+1)t^{\sigma-1}\left(k_1^2(\gamma-\zeta k_1k_2)+\delta k_3^2\right)}{k_1+k_2+k_3}. \tag{71}$$

Then, the system exhibits **neutral stability** ($\mathrm{Re}(\varpi)=0$) for all wavenumbers (k_1, k_2, k_3) satisfying $k_1+k_2+k_3\neq 0$ (see Figures 1-2 ($t = 2$ and $\gamma=\delta=\mu=1$)).

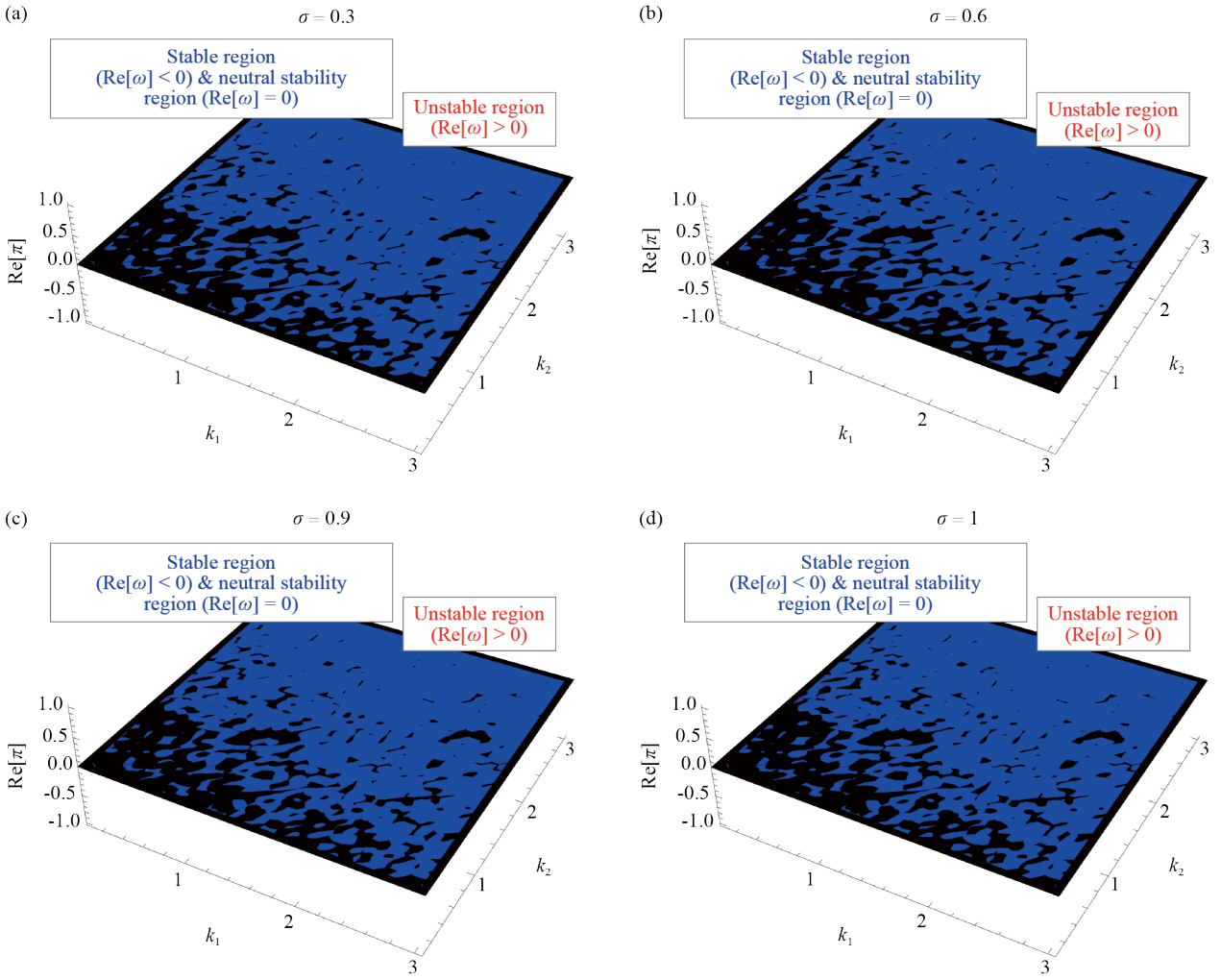

Figure 1. 3D stability diagram for different values of σ showing stable ($\mathrm{Re}[\omega] < 0$), neutral stability ($\mathrm{Re}[\omega] = 0$) and unstable ($\mathrm{Re}[\omega] > 0$) zones with wavenumbers k_1, k_2 when $t = 2$ and $\gamma = \delta = \mu = 1$

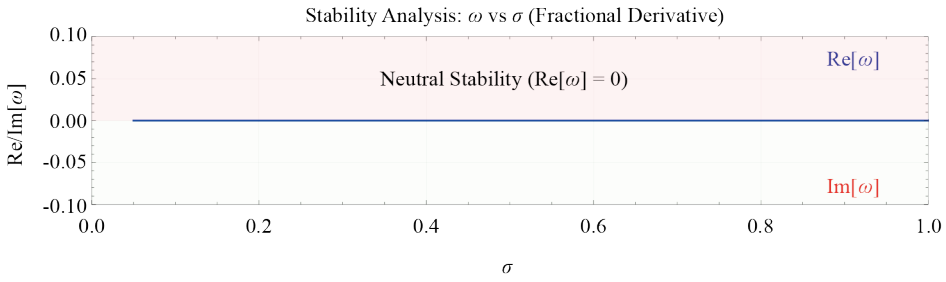

Figure 2. Stability regions showing $\mathrm{Re}[\omega]$ and $\mathrm{Im}[\omega]$ versus σ, with stable ($\mathrm{Re}[\omega] > 0$), neutral stability ($\mathrm{Re}[\omega] = 0$) and unstable ($\mathrm{Re}[\omega] < 0$) zones when $t = 2$ and $\gamma = \delta = \mu = 1$

5. Results and discussion

In this work, we applied the Modified Extended Mapping Method (MEMM) to the fractional (3 + 1)-dimensional Generalized *B*-type Kadomtsev-Petviashvili Equation (GBKPE) and successfully obtained a wide spectrum of exact analytical solutions. The solutions include dark soliton solutions, singular soliton solutions, Jacobi elliptic function solutions, hyperbolic solutions, exponential solutions, and singular periodic solutions. Each of these forms exhibits distinct physical characteristics and potential applications in nonlinear wave dynamics, particularly in plasma physics, fluid mechanics, and nonlinear optics. The obtained dark solitons are characterized by a localized drop in amplitude against a continuous background. Physically, these solutions are important in nonlinear optical systems such as optical fibers, fluid dynamics, and plasma physics. The obtained singular soliton solutions are characterized by a sharp peak or divergence in amplitude at certain points, and they appear in plasma environments and shallow water systems. The obtained Jacobi elliptic function solutions describe periodic wave patterns whose shape depends on the elliptic modulus parameter. These solutions bridge the gap between purely periodic and solitary waveforms, reducing to hyperbolic functions when the modulus approaches unity. Singular periodic solutions exhibit periodic spatial profiles with singularities at certain points within each period. These profiles can be associated with periodic energy focusing or regular occurrence of extreme events in nonlinear systems, such as plasma physics and hydrodynamic systems. Also, the linear stability analysis was performed to assess the robustness of the obtained solutions against small perturbations. By introducing a perturbation into the solution and linearizing the governing equations, the resulting eigenvalue problem was examined. The sign of the real part of the eigenvalues determined the stability criterion: negative real parts indicated that perturbations decay over time, confirming the stability of the solution, whereas positive values implied instability. The analysis revealed that, within the chosen parameter regime, the solutions remain stable under small disturbances, demonstrating their physical relevance and persistence in practical scenarios.

6. Graphical representation for some solutions

This section contains numerical simulations of some gained solutions to show their physical manifestation with three different values for σ. 3-D, contour, and 2-D plots are provided for some of the gained solutions by choosing suitable values of the relevant model parameters. Figure 3 displays the singular periodic solution of Eq. (14) when assuming $\lambda_1 = 0.6$, $\lambda_2 = 0$, $\lambda_3 = 0$, $\gamma = 0.85$, $\zeta = 0.7$, $\beta = 0.75$, $\delta = 0.8$, $\mathfrak{s}_2 = -0.55$, $\omega = 0.65$ and x from -25 to 25. These solutions exhibit periodic oscillations but contain singularities at specific points, representing wave profiles with repeating patterns interrupted by discontinuities or blow-ups. Such behavior often models phenomena like breaking waves or localized instabilities in nonlinear media. Figure 4 displays the dark soliton solution of Eq. (16) when assuming $\lambda_1 = 0.5$, $\lambda_2 = 0$, $\lambda_3 = 0$, $\gamma = 0.8$, $\zeta = 0.6$, $\beta = 0.7$, $\delta = 0.9$, $\mathfrak{s}_2 = 0.55$, $\omega = 0.75$ and x from -20 to 20. These are localized waveforms that appear as dips or voids within a continuous wave background. The dark solitons maintain their shape while propagating and exhibit phase shifts during interactions. They are commonly associated with systems where energy or density is depleted locally, such as in optical fibers or Bose-Einstein condensates. Figure 5 displays the singular soliton solution of Eq. (27) when assuming $\lambda_1 = 0.7$, $\lambda_2 = 0$, $\lambda_3 = 0$, $\gamma = 0.75$, $\zeta = 0.8$, $\beta = 0$, $\delta = 0.85$, $\mathfrak{s}_2 = 0.6$, $\omega = 0.7$ and x from -20 to 20. These solutions combine soliton-like propagation with singularities, representing sharp, localized peaks that move without changing their overall profile but feature blow-ups at finite points. They are often linked to phenomena such as extreme waves or localized energy concentrations in non-linear systems.

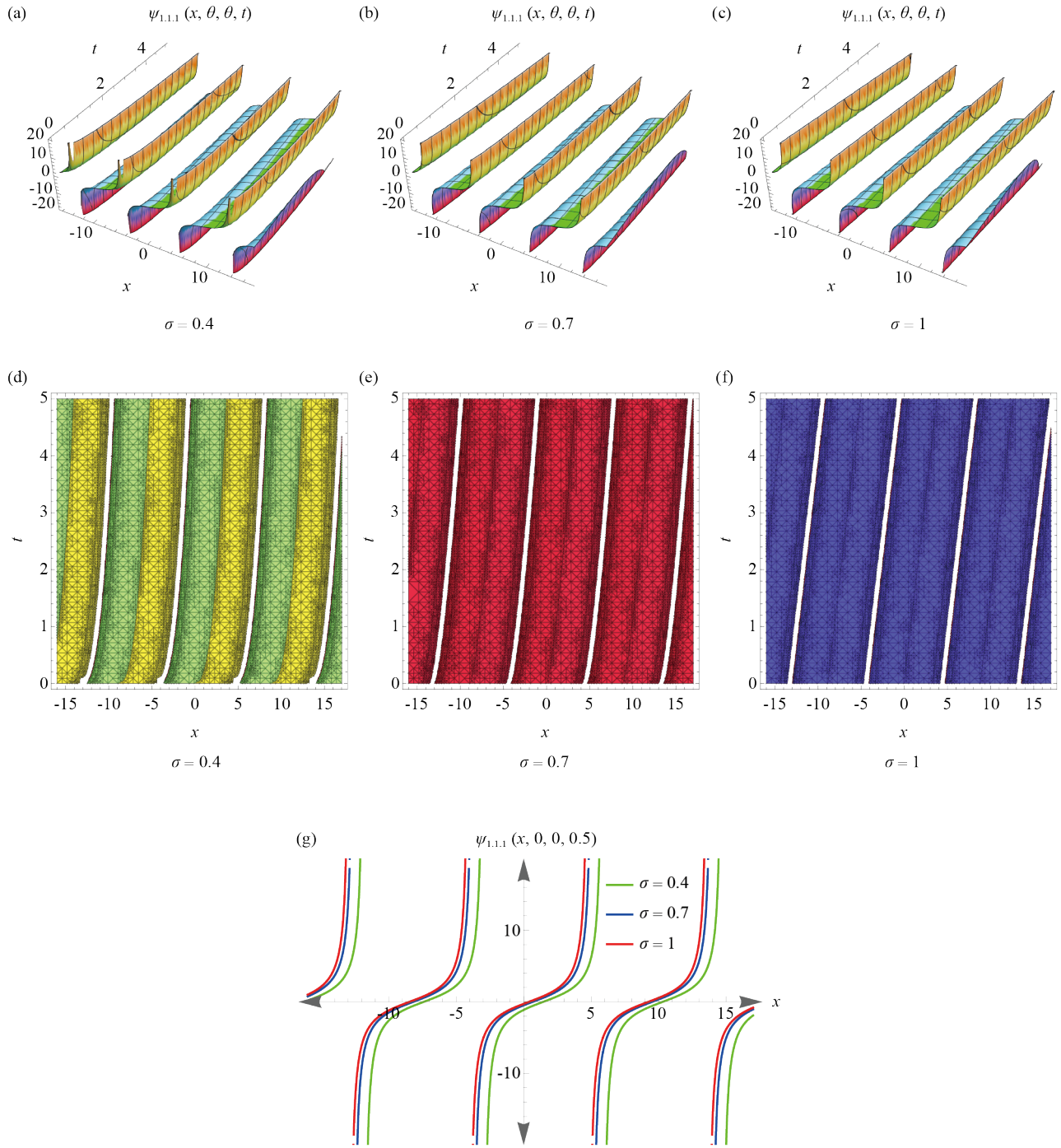

Figure 3. 3D, contour and 2D plots of Eq. (14) at different values of σ when $\lambda_1 = 0.6$, $\lambda_2 = 0$, $\lambda_3 = 0$, $\gamma = 0.85$, $\zeta = 0.7$, $\beta = 0.75$, $\delta = 0.8$, $s_2 = -0.55$, $\omega = 0.65$

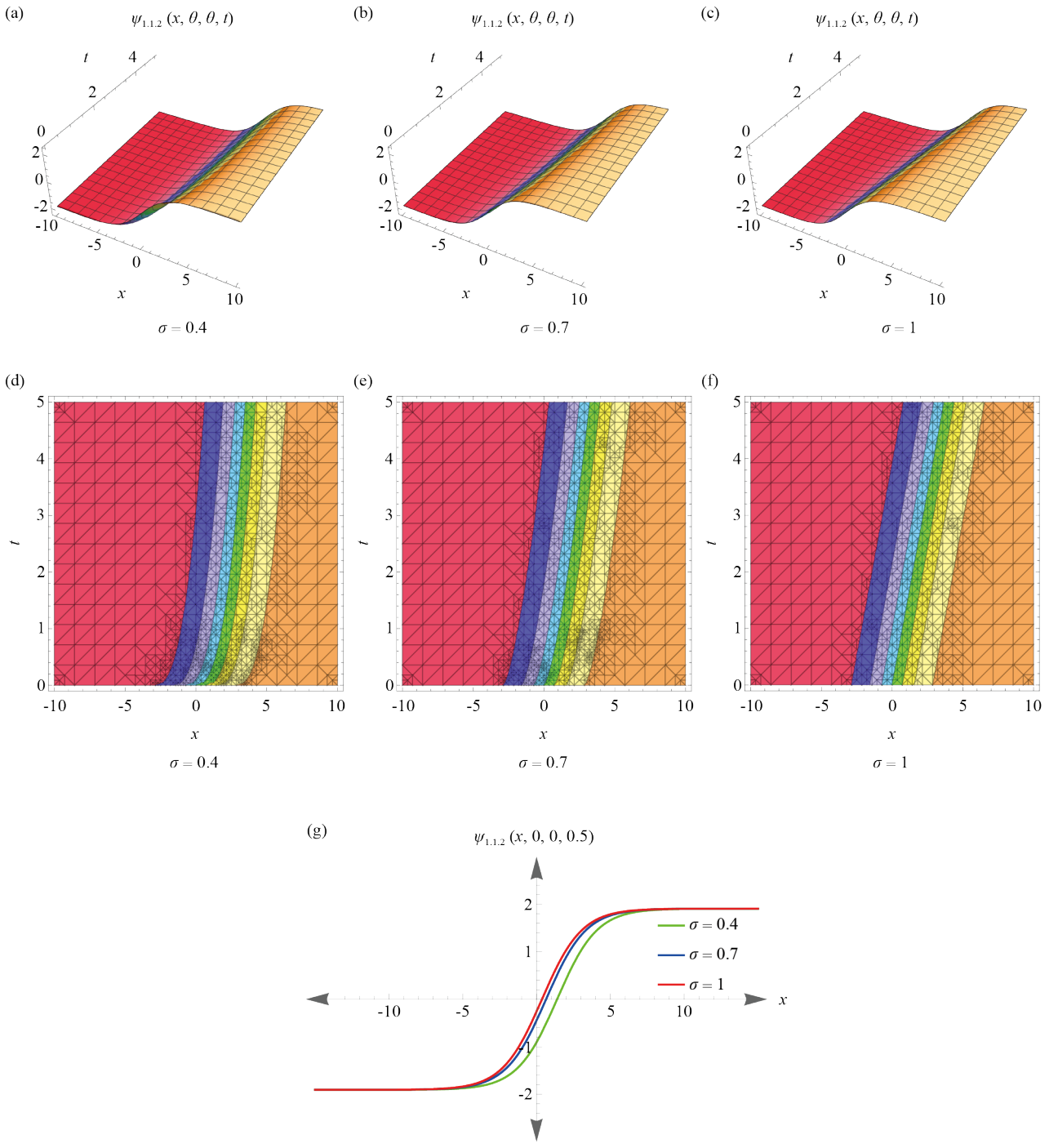

Figure 4. 3D, contour and 2D plots of Eq. (16) at different values of σ when $\lambda_1 = 0.5$, $\lambda_2 = 0$, $\lambda_3 = 0$, $\gamma = 0.8$, $\zeta = 0.6$, $\beta = 0.7$, $\delta = 0.9$, $\mathfrak{s}_2 = 0.55$, $\omega = 0.75$

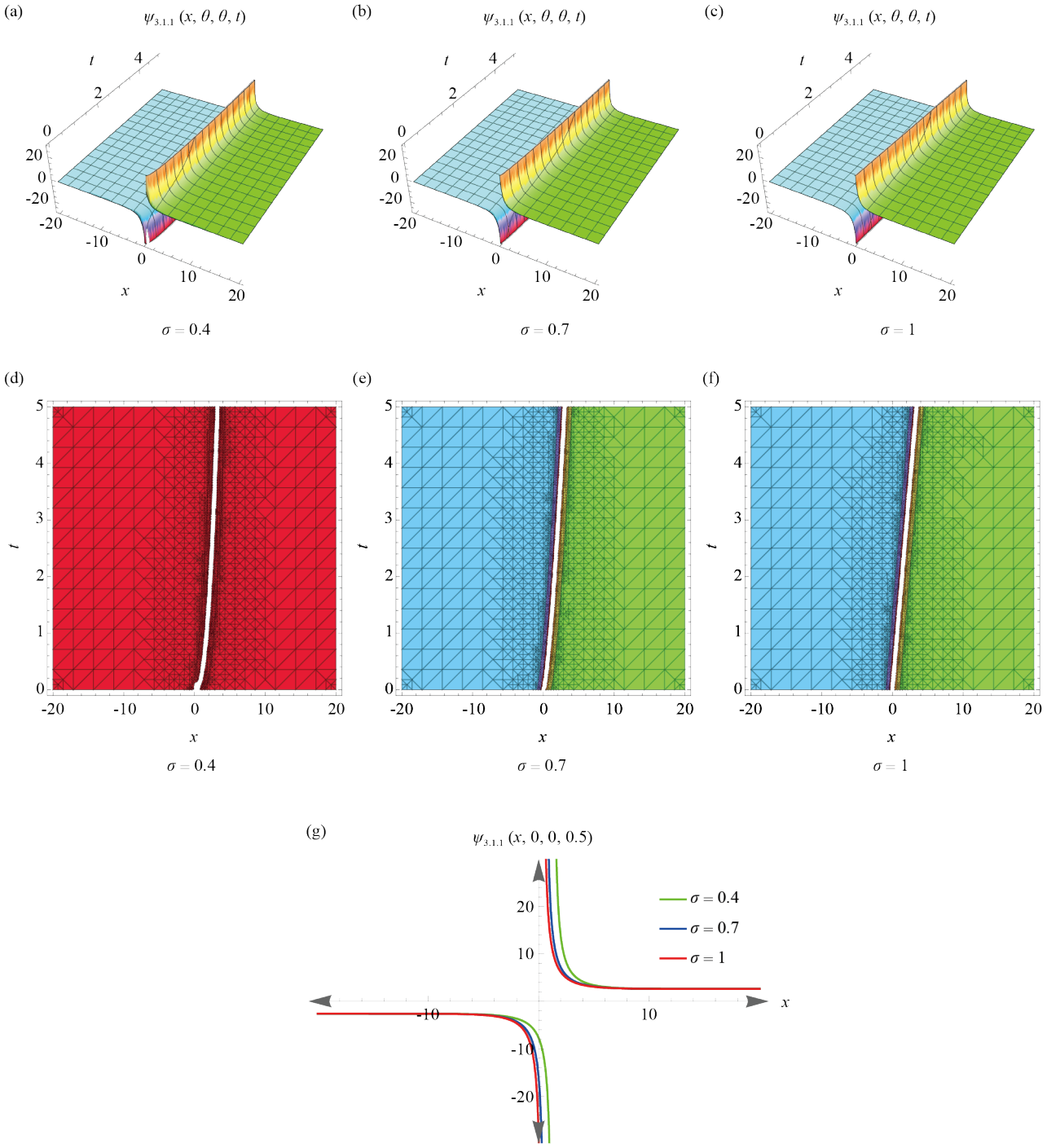

Figure 5. 3D, contour and 2D plots of Eq. (27) at different values of σ when $\lambda_1 = 0.7$, $\lambda_2 = 0$, $\lambda_3 = 0$, $\gamma = 0.75$, $\zeta = 0.8$, $\beta = 0$, $\delta = 0.85$, $s_2 = 0.6$, $\omega = 0.7$

7. Conclusion

In this work, we investigated the fractional (3 + 1)-dimensional generalized *B*-type Kadomtsev-Petviashvili equation, a well-known integrable model in nonlinear wave theory with significant applications in describing wave propagation phenomena in fluid dynamics. The novelty of this study lies in the implementation of the Modified Extended Mapping

Method (MEMM) alongside the local M-fractional derivative, a relatively recent fractional operator that preserves locality while capturing essential memory effects. By employing MEMM under the local M-fractional framework, we successfully derived a wide class of exact solutions, including Jacobi elliptic function solutions, hyperbolic and exponential function solutions, as well as dark and singular soliton solutions. The study of exact and soliton solutions to this equation plays a critical role in understanding the behavior of complex waves. Furthermore, we conducted a linear stability analysis to examine the robustness of the obtained solutions against small perturbations. The stability study confirmed that certain solution classes, particularly the soliton solutions, remain stable under controlled parameter regimes, reinforcing their physical relevance. To illustrate the dynamic behavior and structural properties of the solutions, several representative cases were visualized through contour, 2D, and 3D graphical representations. These findings not only expand the repertoire of known analytical solutions to the fractional nonlinear model but also provide deeper insight into the impact of fractional-order dynamics on wave propagation.

8. Future directions

8.1 *Future recommendations*

Future research can focus on extending the current work by using other forms of fractional derivatives—like conformable fractional derivative or β-fractional derivative—on the (3 + 1)-dimensional generalized B-type Kadomtsev-Petviashvili equation, so that comparisons between solution behaviors in different fractional frameworks can be made. Lastly, the application of the model to real physical systems in plasma physics, fluid dynamics, or nonlinear optics may ascertain its physical validity. Consideration of coupled or further generalized forms of the equation may also yield even richer structures of solutions, like multi-soliton and rogue wave behaviors under the influence of fractional effects.

Conflict of interest

The authors declare no competing financial interest.

References

[1] Biswas A, Milovic D. Bright and dark solitons of the generalized nonlinear Schrödinger's equation. *Communications in Nonlinear Science and Numerical Simulation*. 2010; 15(6): 1473-1484. Available from: https://doi.org/10.1016/j.cnsns.2009.06.017.

[2] Ghayad MS, Badra NM, Ahmed HM, Rabie WB. Derivation of optical solitons and other solutions for nonlinear Schrödinger equation using modified extended direct algebraic method. *Alexandria Engineering Journal*. 2023; 64: 801-811. Available from: https://doi.org/10.1016/j.aej.2022.10.054.

[3] Khalifa AS, Ahmed HM, Badra NM, Rabie WB. Exploring solitons in optical twin-core couplers with Kerr law of nonlinear refractive index using the modified extended direct algebraic method. *Optical and Quantum Electronics*. 2024; 56(6): 1060. Available from: https://doi.org/10.1007/s11082-024-06882-x.

[4] Rabie WB, Ahmed HM. Cubic-quartic solitons perturbation with couplers in optical metamaterials having triple-power law nonlinearity using extended F-expansion method. *Optik*. 2022; 262: 169255. Available from: https://doi.org/10.1016/j.ijleo.2022.169255.

[5] Hosseini K, Alizadeh F, Hinçal E, Ilie M, Osman MS. Bilinear Bäcklund transformation, Lax pair, Painlevé integrability, and different wave structures of a 3D generalized KdV equation. *Nonlinear Dynamics*. 2024; 112: 18397-18411. Available from: https://doi.org/10.1007/s11071-024-09944-7.

[6] Lappalainen K, Piliougine M, Valkealahti S, Spagnuolo G. Photovoltaic module series resistance identification at its maximum power production. *Mathematics and Computers in Simulation*. 2024; 224: 50-62. Available from: https://doi.org/10.1016/j.matcom.2023.05.021.

[7] Özkan YS, Yaşar E, Osman MS. Novel multiple soliton and front wave solutions for the 3D-Vakhnenko-Parkes equation. *Modern Physics Letters B*. 2022; 36(9): 2250003. Available from: https://doi.org/10.1142/S0217984922500038.

[8] Khalifa AS, Badra NM, Ahmed HM, Rabie WB. Retrieval of optical solitons in fiber Bragg gratings for high-order coupled system with arbitrary refractive index. *Optik*. 2023; 287: 171116. Available from: https://doi.org/10.1016/j.ijleo.2023.171116.

[9] Ahmed KK, Badra NM, Ahmed HM, Rabie WB, Mirzazadeh M, Eslami M, et al. Investigation of solitons in magneto-optic waveguides with Kudryashov's law nonlinear refractive index for coupled system of generalized nonlinear Schrödinger's equations using modified extended mapping method. *Nonlinear Analysis: Modelling and Control*. 2024; 29(2): 205-223. Available from: https://doi.org/10.15388/namc.2024.29.34070.

[10] Ghayad MS, Badra NM, Ahmed HM, Rabie WB. Analytic soliton solutions for RKL equation with quadrupled power-law of self-phase modulation using modified extended direct algebraic method. *Journal of Optics*. 2024. Available from: https://doi.org/10.1007/s12596-023-01624-w.

[11] Hosseini K, Alizadeh F, Kheybari S, Hinçal E, Kaymakamzade B, Osman MS. Ginzburg-Landau equations involving different effects and their solitary wave. *Partial Differential Equations in Applied Mathematics*. 2024; 12: 100987. Available from: https://doi.org/10.1016/j.padiff.2024.100987.

[12] Chou D, Rehman HU, Amer A, Osman MS. Optical soliton dynamics of the conformable nonlinear evolution equation in Bose-Einstein condensates. *Lincean Proceedings Physical and Natural Sciences*. 2024; 35: 1065-1076. Available from: https://doi.org/10.1007/s12210-024-01284-3.

[13] Osman MS, Rezazadeh H, Eslami M. Traveling wave solutions for (3 + 1) dimensional conformable fractional Zakharov-Kuznetsov equation with power law nonlinearity. *Nonlinear Engineering*. 2019; 8(1): 559-567. Available from: https://doi.org/10.1515/nleng-2018-0163.

[14] Akinyemi L, Houwe A, Abbagari S, Wazwaz AM, Alshehri HM, Osman MS. Effects of the higher-order dispersion on solitary waves and modulation instability in a monomode fiber. *Optik*. 2023; 288: 171202. Available from: https://doi.org/10.1016/j.ijleo.2023.171202.

[15] Akbar MA, Abdullah FA, Islam MT, Al Sharif MA, Osman MS. New solutions of the soliton type of shallow water waves and superconductivity models. *Results in Physics*. 2023; 44: 106180. Available from: https://doi.org/10.1016/j.rinp.2022.106180.

[16] Ghayad MS, Ahmed HM, Badra NM, Rabie WB. Wave propagation analysis of the fractional generalized (3 + 1)-dimensional *P*-type equation with local *M*-derivative. *Journal of Umm Al-Qura University for Applied Sciences*. 2025. Available from: https://doi.org/10.1007/s43994-025-00238-1.

[17] Ghosh B, Manda S. Fiber Bragg grating-based optical filters for high-resolution sensing: A comprehensive analysis. *Results in Optics*. 2023; 12: 100441. Available from: https://doi.org/10.1016/j.rio.2023.100441.

[18] Ghayad MS, Ahmed HM, Badra NM, Rezazadeh H, Hosseinzadeh MA, Rabie WB. Extraction of new optical solitons of conformable time fractional generalized RKL equation via quadrupled power-law of self-phase modulation. *Optical and Quantum Electronics*. 2024; 56: 1304. Available from: https://doi.org/10.1007/s11082-024-06938-y.

[19] Agathiyan A, Gowrisankar A, Fataf NAA, Cao J. Remarks on the integral transform of non-linear fractal interpolation functions. *Chaos, Solitons & Fractals*. 2023; 173: 113749. Available from: https://doi.org/10.1016/j.chaos.2023.113749.

[20] Ahmed KK, Badra NM, Ahmed HM, Rabie WB. Soliton solutions of generalized Kundu-Eckhaus equation with an extra-dispersion via improved modified extended tanh-function technique. *Optical and Quantum Electronics*. 2023; 55: 1-17. Available from: https://doi.org/10.1007/s11082-023-04599-x.

[21] Tripathy A, Sahoo S, Rezazadeh H, İzgi ZP, Osman MS. Dynamics of damped and undamped wave natures in ferromagnetic materials. *Optik*. 2023; 281: 170817. Available from: https://doi.org/10.1016/j.ijleo.2023.170817.

[22] Ahmed KK, Badra NM, Ahmed HM, Rabie WB. Soliton solutions and other solutions for Kundu-Eckhaus equation with quintic nonlinearity and Raman effect using the improved modified extended Tanh-Function method. *Mathematics*. 2022; 10(22): 4203. Available from: https://doi.org/10.3390/math10224203.

[23] Gao XY. Bäcklund transformation and shock-wave-type solutions for a generalized (3 + 1)-dimensional variable-coefficient *B*-type Kadomtsev-Petviashvili equation in fluid mechanics. *Ocean Engineering*. 2015; 96: 245-247. Available from: https://doi.org/10.1016/j.oceaneng.2014.12.017.

[24] Ghayad MS, Badra NM, Ahmed HM, Rabie WB, Mirzazadeh M, Hashemi MS. Highly dispersive optical solitons in fiber Bragg gratings with cubic quadratic nonlinearity using improved modified extended tanh-function method. *Optical and Quantum Electronics*. 2024; 56: 1184. Available from: https://doi.org/10.1007/s11082-024-07064-5.

[25] Yusuf A, Sulaiman TA, Inc M, Bayram M. Breather wave, lump-periodic solutions and some other interaction phenomena to the Caudrey-Dodd-Gibbon equation. *European Physical Journal Plus*. 2020; 135: 563. Available from: https://doi.org/10.1140/epjp/s13360-020-00566-7.

[26] Atangana A, Secer A. A note on fractional order derivatives and table of fractional derivatives of some special functions. *Abstract and Applied Analysis*. 2013. Available from: https://doi.org/10.1155/2013/279681.

[27] Tarasov VE, Tarasova SS. Fractional derivatives and integrals: what are they needed for? *Mathematics*. 2020; 8(2): 164. Available from: https://doi.org/10.3390/math8020164.

[28] Agathiyan A, Fataf NAA, Gowrisankar A. Explicit relation between Fourier transform and fractal dimension of fractal interpolation functions. *The European Physical Journal Special Topics*. 2023; 232(7): 1077-1091. Available from: https://doi.org/10.1140/epjs/s11734-023-00779-8.

[29] Caputo M. Linear models of dissipation whose Q is almost frequency independent-II. *Geophysical Journal International*. 1967; 13(5): 529-539. Available from: https://doi.org/10.1111/j.1365-246X.1967.tb02303.x.

[30] Kilbas AA. Hadamard-type fractional calculus. *Journal of the Korean Mathematical Society*. 2001; 38(6): 1191-1204.

[31] Khalil R, Al Horani M, Yousef A, Sababheh M. A new definition of fractional derivative. *Journal of Computational and Applied Mathematics*. 2014; 264: 65-70. Available from: https://doi.org/10.1016/j.cam.2014.01.002.

[32] Soliman M, Ahmed HM, Badra N, Ramadan ME, Samir I, Alkhatib S. Influence of the β-fractional derivative on optical soliton solutions of the pure-quartic nonlinear Schrödinger equation with weak nonlocality. *AIMS Mathematics*. 2025; 10(3): 7489-7508.

[33] Sousa JVDC, de Oliveira EC. M-fractional derivative with classical properties. *arXiv:170408186*. 2017. Available from: https://arxiv.org/abs/1704.08186.

[34] Alaoui MK, Uddin M, Roshid MM, Roshid HO, Osman MS. Modulation instability, and dynamical behavior of solitary wave solution of time M-fractional Clannish Random Walker's Parabolic equation via two analytic techniques. *Partial Differential Equations in Applied Mathematics*. 2024; 12: 101011. Available from: https://doi.org/10.1016/j.padiff.2024.101011.

[35] Mahdy AM. Stability, existence, and uniqueness for solving fractional glioblastoma multiforme using a Caputo-Fabrizio derivative. *Mathematical Methods in the Applied Sciences*. 2025; 48(7): 7360-7377. Available from: https://doi.org/10.1002/mma.9038.

[36] Raza N, Osman MS, Abdel-Aty A, Abdel-Khalek S, Besbes H. Optical solitons of space-time fractional Fokas-Lenells equation with two versatile integration architectures. *Advances in Difference Equations*. 2020; 2020: 517. Available from: https://doi.org/10.1186/s13662-020-02973-7.

[37] Song L, Zhang H. Solving the fractional BBM-Burgers equation using the homotopy analysis method. *Chaos, Solitons and Fractals*. 2009; 40(4): 1616-1622. Available from: https://doi.org/10.1016/j.chaos.2007.09.042.

[38] Guy J. Lagrange characteristic method for solving a class of nonlinear partial differential equations of fractional order. *Applied Mathematics Letters*. 2006; 19(9): 873-880. Available from: https://doi.org/10.1016/j.aml.2005.10.016.

[39] Zayed EME. A note on the modified simple equation method applied to Sharma-Tasso-Olver equation. *Applied Mathematics and Computation*. 2011; 218(7): 3962-3964. Available from: https://doi.org/10.1016/j.amc.2011.09.025.

[40] Odibat ZM, Momani S. Fractional Green function for linear time-fractional equations of fractional order. *Journal of Applied Mathematics and Computing*. 2007; 24(1): 167-178. Available from: https://doi.org/10.1007/BF02832308.

[41] Tarla S, Ali KK, Yilmazer R, Osman MS. New optical solitons based on the perturbed Chen-Lee-Liu model through Jacobi elliptic function method. *Optical and Quantum Electronics*. 2022; 54(2): 131. Available from: https://doi.org/10.1007/s11082-022-03527-9.

[42] Ma YX, Tian B, Qu QX, Wei CC, Zhao X. Bäcklund transformations, kink soliton, breather- and travelling-wave solutions for a (3 + 1)-dimensional B-type Kadomtsev-Petviashvili equation in fluid dynamics. *Chinese Journal of Physics*. 2021; 73: 600-612. Available from: https://doi.org/10.1016/j.cjph.2021.07.001.

[43] Tu JM, Tian SF, Xu MJ, Ma PL, Zhang TT. On periodic wave asymptotic behaviors to a (3 + 1)-dimensional B-type Kadomtsev-Petviashvili equation in fluid dynamics. *Computers & Mathematics with Applications*. 2016; 72(9): 2486-2504. Available from: https://doi.org/10.1016/j.camwa.2016.09.003.

[44] Ghayad MS, Ahmed HM, Badra NM, Rezazadeh H, Hosseinzadeh MA, Rabie WB. New analytical wave structures for generalized *B*-type Kadomtsev-Petviashvili equation by improved modified extended tanh function method. *Physica Scripta*. 2024; 99(12): 125224. Available from: https://doi.org/10.1088/1402-4896/ad8aa4.

[45] Yan XW, Tian SF, Wang XB, Zhang TT. Solitons to rogue waves transition, lump solutions and interaction solutions for the (3 + 1)-dimensional generalized *B*-type Kadomtsev-Petviashvili equation in fluid dynamics. *International Journal of Computer Mathematics*. 2019; 96: 1839-1848. Available from: https://doi.org/10.1080/00207160.2018.1535708.

[46] Ahmed KK, Ahmed HM, Badra NM, Mirzazadeh M, Rabie WB, Eslami M. Diverse exact solutions to Davey-Stewartson model using modified extended mapping method. *Nonlinear Analysis: Modelling and Control*. 2024; 29: 983-1002. Available from: https://doi.org/10.15388/namc.2024.29.36103.

[47] Arshad M, Seadawy AR, Lu D. Modulation stability and dispersive optical soliton solutions of higher order nonlinear Schrödinger equation and its applications in mono-mode optical fibers. *Superlattices and Microstructures*. 2018; 113: 419-429. Available from: https://doi.org/10.1016/j.spmi.2017.11.022.